THE IMPACT OF HIGH DIETARY GLUCOSE ON AMYLOID-BETA PROTEOTOXICITY IN *CAENORHABDITIS ELEGANS*

by

Emylee Ann Kerslake

A thesis submitted to the Faculty of the University of Delaware in partial fulfillment of the requirements for the degree of Master of Science in Biological Sciences

Summer 2024

THE IMPACT OF HIGH DIETARY GLUCOSE ON AMYLOID-BETA PROTEOTOXICITY IN *CAENORHABDITIS ELEGANS*

by

Emylee Ann Kerslake

Approved: _____

Jessica Tanis, Ph.D.
Professor in charge of thesis on behalf of the Advisory Committee

Approved: _____

Velia Fowler, Ph.D.
Chairman for the Department of Biological Sciences

Approved: _____

Debra Hess Norris
Interim Dean of the College of Arts and Sciences

Approved: _____

Louis F. Rossi, Ph.D.
Vice Provost for Graduate and Professional Education and
Dean of the Graduate College

ACKNOWLEDGMENTS

I am forever indebted to several individuals for their support, wisdom, and compassion throughout my graduate experience. First and foremost, I am so grateful to have such an incredible mentor in Dr. Jessica Tanis. Her continued understanding and candor has pushed me to become not only a better scientist, but also communicator, colleague, and friend. Being a part of the Tanis Lab has brought such incredible people into my life, all of whom deserve recognition for their assistance these past three years. An enormous thank you to our current lab members: Malek Elsayyid, Karli Sunnergren, Nahin Siara Prova, Alexis Semmel, Tao Ke, Rachel Wang, Aaurshii Taneja, McKenna Miller, and Krisha Parekh; as well as those who have moved on during my time here: Dr. Andy Lam, Dr. Michael Clupper, Dr. Denis Touroutine, Katherine Wagner, Carter O'Brien, John Salsini-Tobias, and Allison Davis. Getting to know each of you has been such a rewarding experience. I cannot express enough the depth of gratitude I hold for everyone, but especially to my mentor Dr. Andy Lam. Thank you for teaching me everything I needed and for your continued support throughout my trials, even after graduating. I am grateful for my thesis committee members Dr. Jaramillo-Lambert and Dr. Shao for their encouragement and advice, as well as the UD Worm Club community. Thank you to the University of Delaware and the Biological Sciences Graduate department for giving me the opportunity and resources to conduct research and earn a Graduate degree; including the honor of being selected for the Graduate Scholars Award. Last but not least is a thank you to my friends and family who have supported, encouraged, and cheered me on throughout this journey. Your unconditional loyalty does not go unnoticed or unappreciated… and to my grandma, Mary Spencer Kerslake, who wanted so badly to be here on my graduation day but just couldn't hold on that long… I love you. I know you would be proud.

TABLE OF CONTENTS

LIST OF FIGURES VI

LIST OF TABLES XI

ABSTRACT XII

Chapter

1 INTRODUCTION 1

1.1 Alzheimer's Disease 1

1.1.1 Pathophysiology 2

1.1.1.1 Amyloid-Beta Proteotoxicity 3
1.1.1.2 Oxidative Stress 6
1.1.1.3 Bioenergetic Defects 8
1.1.1.4 Impaired Glucose Metabolism 10

1.1.2 Risk Factors 13

1.2 The Role of Diet in Disease 15
1.3 *Caenorhabditis elegans* as a Model for AD 16
1.4 Aims and Hypothesis 19

2 METHODS 21

2.1 Nematode Culture 21
2.2 Bacterial strains 22
2.3 Creating Strains 23
2.4 Aβ-induced Paralysis Assay 23
2.5 ATP and ROS Quantification 24
2.6 Glucose Quantitation Assay 25

3 RESULTS 27

3.1 Analysis of Aβ Supplemented with High Dietary Glucose and Vitamin B_{12} 27
3.2 Analysis of *fgt-2* Mutants Expressing Aβ, Supplemented with High Dietary Glucose and Vitamin B_{12} 31
3.3 Analysis of Aβ; *fgt-1* and Aβ; *fgt-1*;*fgt-2* Animals Supplemented with High Dietary Glucose 40

4 DISCUSSION.....49
REFERENCES.....55

LIST OF FIGURES

Figure 1: Non-Amyloidogenic vs. Amyloidogenic APP Processing (Hampel et al., 2018). BACE1= APP. **6**

Figure 2: Oxidative Stress Model in Alzheimer's Pathology (Chen & Zhong, 2014). The disease pathologies and modalities associated in Alzheimer's Disease and their impact on other features. **10**

Figure 3: Glucose and Lactate Uptake Pathway (Koepsell, 2020). D-glucose and L-lactate uptake pathways via transporter activity from blood to nerve cells. In times of fasting or low-sugar diets such as the Ketogenic Diet, cells derive ATP from lactate provided either from blood or astrocytes directly. **13**

Figure 4: Time-Dependent Paralysis of Aβ Animals. Graphical representation of the % of moving animals after Aβ-expression is induced. Animals are placed at 25 degrees C at the end of larval stage 4 (L4). **18**

Figure 5: Human versus *C. elegans* Nutrient Absorption (Yilmaz & Walhout, 2014). Translational model of dietary nutrient absorption between humans and *C. elegans*. **19**

Figure 6: Glucose-induced Accelerated Paralysis Negated by HB101 *E. coli* Diet. 10mM glucose supplementation (gray) leads to a dietary shift – an accelerated time-to-paralysis was observed compared to OP50 fed animals (black). HB101 fed animals (red) and glucose supplemented animals (pink) have a delay in time-to-paralysis and removal of the dietary shift. Median paralysis times are shown in parenthesis. **20**

Figure 7: Vitamin B_{12} Provides Slight Protection Against High Dietary Glucose Increased Time-To-Paralysis. Aβ worms grown on agar plates supplemented with either B_{12}, 10mM Glucose, or B_{12}+10mM Glucose and seeded with one of two *E. coli* bacterial cultures: OP50 (solid lines) or HB101 (dashed lines). Median paralysis times are shown in parentheses (). **29**

Figure 8: Vitamin B_{12} Protects Against ROS Accumulation from High Dietary Glucose. Aβ worms grown on agar plates supplemented with either vitamin B_{12}, 10mM glucose, or both; all plates were seeded with OP50 *E. coli* bacterial culture. Vitamin B_{12} (pink) had a significant decrease in H_2O_2 accumulation (*$p<0.05$), while 10mM glucose (teal) had a

significant increase (****p<0.0001) that was restored when supplemented with vitamin B_{12} (purple). n<4 **29**

Figure 9: High Dietary Glucose Has No Impact on ATP Levels. Aβ animals grown on either NGM (black) or 10mM glucose (pink) agar plates. Ns=not significant, n=3. **30**

Figure 10: Differentially Regulated Genes Between OP50 and HB101 fed Animals. RNAseq data showcasing a sample of significantly upregulated genes in OP50 fed animals compared to HB101. n=3. **31**

Figure 11: Loss of *fgt-2* Delays Aβ-induced Time-to-Paralysis. Control animals fed HB101 (grey dashed) induce a significant dietary shift compared to control animals fed OP50 (black solid). Loss of *fgt-2* removes the shift between the two diets; OP50 fed mutants (blue solid) and HB101 fed mutants (blue dashed) median time-to-paralysis act comparable to the HB101 control (grey dashed). **32**

Figure 12: Loss of *fgt-2* Removes the Detrimental Impact of Glucose on Aβ-Induced Paralysis. Mutant animals grown on OP50+10mM glucose (blue dashed) exhibit elimination of the dietary shift caused by excessive glucose when compared to OP50 mutant animals (blue solid). On average, HB101+10mM glucose mutants (green solid) showcase a slight delay in median paralysis when compared to the OP50+10mM glucose mutants (blue dashed), but not HB101+10mM glucose control animals (red solid). **33**

Figure 13: Loss of *fgt-2* Removes the Dietary Shift caused by Glucose in OP50. Mutant animals grown on 10mM glucose (teal) have a median time-to-paralysis similar to those grown on NGM control (pink). Control animals grown on NGM (grey) experience a significant acceleration in time-to-paralysis (***p<0.0005) compared to mutants (pink). Control animals grown on 10mM glucose (blue) exhibit the usual acceleration (**p<0.005) compared to control grown on NGM (grey). n<3. **34**

Figure 14: Control versus *fgt-2* Median Paralysis on OP50 and HB101. (A) Graphical comparison between total median time-to-paralysis for control and mutant animals grown on 10mM glucose seeded with either OP50 or HB101. Control animals exhibit a dietary shift (**p<0.005) between the two *E. coli* strains. Loss of *fgt-2*, while overall delaying the time-to-paralysis (**p<0.005) compared to control, fails to completely remove the dietary shift between OP50 and HB101 when supplemented with

10mM glucose. Control and mutant worms fed HB101+10mM glucose have no significant change in time-to-paralysis. n<3. (B) Graphical comparison of total median time-to-paralysis for *fgt-2* mutants on all conditions. Loss of *fgt-2* removes the dietary shift between OP50 and HB101 but fails to remove this when excess glucose is present (**p<0.005). n<3. **35**

Figure 15: Loss of *fgt-2* Impacts ROS Accumulation and ATP Levels. (A) Graphical comparison of hydrogen peroxide levels between control and *fgt-2* mutants (+/-) 10mM glucose. Control animals supplemented 10mM glucose showcase significantly higher (****p<0.0001) ROS accumulation versus control and mutant animals. Loss of *fgt-2* restored control values. n<3. (B) Graphical comparison of ATP levels between control and *fgt-2* mutants (+/-) 10mM glucose. Control animals show no significant change with or without glucose supplementation. *fgt-2* mutants ATP levels were significantly higher (*p<0.05) than the control with no significance when supplementing glucose. n=2. **36**

Figure 16: B_{12} Supplementation on *fgt-2* Mutants Negatively Impacts ROS and ATP Levels. (A) Graphical comparison of hydrogen peroxide levels for *fgt-2* mutants on various supplementation conditions. B_{12} supplementation resulted in a significant (*p<0.05) increase in H_2O_2 when paired with 10mM glucose. No significance was seen between control and 10mM glucose. n=2. (B) Graph showcases the comparison of ATP levels in *fgt-2* mutants grown on various supplementation plates. Animals grown on B_{12} + 10mM glucose saw a significant decrease (*p<0.05) in ATP compared to the 10mM glucose. Not enough trials were performed to determine significance for NGM and B_{12} plates. **38**

Figure 17: *fgt-2* Promoter::mScarlet Tag Reveals Intestinal and Muscular Expression Pattern. Images captured using L4 and adult worms paralyzed using levamisole and staged on agarose pads. Imaris ImageJ used for analysis and color-blind recoloring. Andor Spinning Disk Dragonfly Confocal Microscope was used at 10x magnification 10% fluorescence intensity. **39**

Figure 18: *fgt-2* Promoter::mScarlet Tag Reveals Neuronal Expression Pattern. Images captured using L4 and adult worms paralyzed using levamisole and staged on agarose pads. Imaris ImageJ used for analysis and color-blind recoloring. Andor Spinning Disk Dragonfly Confocal Microscope was used at 10x magnification and 10% fluorescence intensity. **40**

Figure 19: Loss of *fgt-1* Median Paralysis on OP50. Graphical comparison of median time-to-paralysis of control animals versus *fgt-1* mutants (+/-) 10mM glucose. Loss of *fgt-1* causes a significant acceleration (*p<0.05) in time-to-paralysis compared to the control. Control animals fed 10mM glucose see a significant decrease in median paralysis (**p<0.005) compared to control but see no significant difference from *fgt-1* mutants. n<3. **42**

Figure 20: Loss of *fgt*-1 Eliminates the Dietary Shift between OP50 and HB101 *E. coli*. Mutant animals fed OP50 *E. coli* (black) present with a similar time-to-paralysis as HB101 (red). HB101 is accelerated compared to previous data and is restored when animals are supplemented with glucose (dashed red). **42**

Figure 21: Loss of *fgt-1* Negates Beneficial Impact of HB101 Diet. Knockout animals remove the dietary shift seen between the two strains of *E. coli.* Addition of 10mM glucose to agar plates seeded with HB101 bacteria restores the protective impact against proteotoxicity (*p<0.05). n=3. **43**

Figure 22: Loss of *fgt-1* Fails to Remove Glucose-Induced Dietary Shift. (A) Graphical comparison of median time-to-paralysis between *fgt-1* and *fgt-2* mutants on 10mM glucose on both *E. coli* diets. Loss of *fgt-1* fails to remove the dietary shift between the strains (*p<0.05). HB101 fed *fgt-1* mutants perform similar to OP50 fed *fgt-2* mutants, while *fgt-2* mutants experience a significant difference between the two bacterial diets (**p<0.005). n=3. (B) Graphical comparison of median time-to-paralysis between control animals and *fgt-1* mutants on glucose. Control animals perform similar to mutants on OP50 and see a dietary shift when fed HB101 *E. coli* (**p<0.005). Mutants fail to remove this shift between the strains (*p<0.05). n=3. **44**

Figure 23: Loss of *fgt-1* and *fgt-2* Causes Paralysis Similar to *fgt-1* Mutant. Paralysis experimentation showcased that loss of both glucose transporters presents with the *fgt-1* phenotype. Double mutants (purple) paralyzed similar to *fgt-1* mutants (pink). **45**

Figure 24: Glucose Must be Metabolized by *C. elegans* to Induce a Shift. Aβ animals grown on NGM agar plates seeded with OP50 *E. coli* were directly grown with nutrient supplementation before seeding. **47**

Figure 25: Glucose Supplementation had No Impact on Total Body Glucose. (A) Total body glucose in animals grown on plates seeded with OP50 bacterial

culture. *fgt-1* mutants are significantly higher levels of glucose compared to *fgt-2* (*p<0.05). n=2. (B) Total body glucose in animals grown on plates seeded with OP50 + 100mM glucose bacterial culture. n=2. **48**

LIST OF TABLES

Table 1: Completed *C. elegans* Mutant Strain Information. *C. elegans* strains generated and used for subsequent experimentation. [1]Tokyo, Japan International *C. elegans* Knockout Consortium (Barstead et al., 2012). **22**

ABSTRACT

Alzheimer's disease (AD) is the leading neurodegenerative disorder worldwide, with an estimated 60 million individuals currently afflicted. Pathological features of this debilitating condition include amyloid-beta (Aβ) accumulation, bioenergetic defects, increased oxidative stress, and impaired glucose metabolism. Since there is currently no disease-modifying treatment for AD, it is essential to understand how modifiable risk factors such as diet impact disease onset and progression. It is difficult to determine the impact of specific nutrients in humans due to complex diet, organismal complexity, genetic diversity, and indirect effects of the gut microbiome. Individuals with abnormal blood sugar levels and glucose utilization are at greater risk for AD, likely because glucose is required to fuel neuronal function. Yet we lack an understanding of how the interplay between glucose and other macro/micronutrient availability impacts brain health. To investigate the effect of excess sugar on amyloid-beta proteotoxicity, I used a transgenic strain of *C. elegans* expressing the toxic human $A\beta_{1-42}$ peptide in the body wall muscles, which produces AD-like pathogenic features such as a time-dependent paralysis that mimics progression of the disease, reduced ATP levels, and increased reactive oxygen species. We discovered that glucose supplementation accelerated paralysis in Aβ animals that consumed OP50 *E. coli* yet had no effect on worms fed HB101 *E. coli*. While vitamin B_{12} can protect against Aβ-

induced proteotoxicity, B_{12} is not the factor in the HB101 diet that nullifies the toxic effects of excess glucose levels. To determine how this diet was protective we performed RNA-Seq and observed downregulation of the predicted facilitated glucose transporter *F14E5.1 (fgt-2)* in animals fed HB101. Loss of *fgt-2* slowed Aβ-induced paralysis, alleviated bioenergetic defects, and reduced ROS accumulation in Aβ animals fed OP50. In the presence of excess glucose, the *fgt-2(tm3206)* mutation abrogated accelerated Aβ-induced paralysis, resulting in a similar time to paralysis regardless of the diet consumed. These findings suggest that *fgt-2* impacts Aβ-induced proteotoxicity, potentially by modulating glucose metabolism via glucose transporter availability. However, *fgt-2* is not the primary glucose transporter in *C. elegans*, and its function is not entirely known. In order to further investigate the significance of glycolytic transport in Aβ-induced proteotoxicity, I crossed the Aβ transgene with *fgt-1*, the primary glucose transporter. Loss of *fgt-1* resulted in an accelerated time to paralysis, suggesting the importance of the role glucose import plays. Loss of both *fgt-1* and *fgt-2* produces a similar result to the *fgt-1* single mutant, indicating that either the protective effects of *fgt-2* rely on *fgt-1* or the function of the primary glucose transporter is crucial regardless of protection elsewhere. Overall, my research highlights the importance of glycolytic transport for overall well-being while demonstrating the impact excess sugar intake has on disease pathologies.

Chapter 1 INTRODUCTION

1.1 Alzheimer's Disease

Alzheimer's Disease (AD) is a progressive neurodegenerative disorder marked as the primary perpetrator of dementia, estimated to be responsible for 50-70% of cases worldwide (Zhang et al., 2021). According to the National Alzheimer's Association, 6.7 million Americans alone are living with the disease in 2023, with 73% of those individuals aged 75 and above. Characteristic symptoms of Alzheimer's include cognitive decline in various domains such as language, memory, executive function, and visuospatial awareness. Severity of symptoms can vary from individual to individual, however the loss of basic cognitive function remains debilitating for patients and caregivers alike. AD is multifactorial in nature, suggesting there are various pathologies that amalgamate to produce the disease as we know it today. In order to reach a definitive diagnosis, doctors used to require post-mortem evaluation of brain tissue in addition to other biomarkers such as cerebral spinal fluid (CSF) or positron emission tomography (PET) due to the similarities AD patients share with other forms of dementia (Budson & Solomon, 2012). In more recent years, however, the emergence of newer detection technologies has made non-invasive techniques more reliable and effective. There are two hallmark features necessary for reaching a clinical diagnosis of AD: a rise in senile extracellular amyloid-beta (Aβ) plaque

formation and intracellular neurofibrillary tangles (NFTs) via hyperphosphorylated tau aggregation (Weller & Budson, 2018). Through the use of a radiolabeled tracer agent, doctors can detect amyloid-beta plaque deposits via a specialized PET scan with 96% sensitivity and 100% specificity (Weller & Budson, 2018).

1.1.1 Pathophysiology

Despite ongoing research efforts, a definitive disease modifying treatment remains elusive due to the complexity of Alzheimer's pathophysiology. Research has, however, found several genetic anomalies implicated in disease pathogenesis. Dominantly inherited familial AD (FAD) has been linked to mutations in genes that encode for the amyloid precursor protein (*APP*), presenilin 1 (*PSEN1)* and presenilin 2 (*PSEN2);* however, these individuals only account for 1% of total Alzheimer's patients (Deture & Dickson, 2019). Specific polymorphisms in the apolipoprotein E gene *(APOE)* are a risk factor for developing late-onset AD, with the risk ratio rising depending on hetero- or homozygous allele possession (Lane et al., 2018). There is significant evidence suggests that over 70 genes affect risk of AD, including TREM2, ADAM10, PLD3 (King et al., 2019). While many of these genes are directly involved in either amyloid-beta formation or tau aggregation, several others with known functionality encode for proteins or enzymes that impact immune response, endocytosis, and cholesterol metabolism (Karch & Goate, 2015)(Jansen et al., 2019).

While there is a small group of individuals who possess hereditary mutations, 80-90% of Alzheimer's patients are late-onset and idiopathic (Reitz et al., 2020).

Without any indication as to how this disease arises in these patients, targeted therapies and prevention methods remain at a standstill. However, the rise of personalized medicine and genetic testing has opened the door to dissecting multifactorial diseases such as AD by providing insight into other metabolic processes differentially regulated through pathogenesis; most of which were previously unknown. Genetic contributions and downstream effector's roles in influencing disease are now a lucrative area of study for complex conditions like Alzheimer's and will be used to create a roadmap towards a potential cure.

1.1.1.1 Amyloid-Beta Proteotoxicity

Proper function of *APP, PSEN1,* and *PSEN2* is vital, as these genes play a critical role in one recognized pathology of Alzheimer's Disease – Aβ proteotoxicity. Amyloid-beta proteotoxicity is characterized as the abnormal aggregation of extracellular amyloid-β into plaques throughout the brain. Plaques form via aberrant proteolytic cleavage of the amyloid precursor protein – a naturally occurring single-pass transmembrane protein containing a long extracellular N-terminus domain and a short intracellular C-terminus tail domain (Hampel et al., 2018; Hardy & Allsop, 1991; Hardy & Selkoe, 2002). β-secretase cleaves off a large extracellular ectodomain, $sAPP_{\beta}$, before the intramembranous γ-secretase catalytic subunit – containing either presenilin 1 or presenilin 2 – removes the amyloid intracellular domain, resulting in a small soluble Aβ peptide **(Figure 1)**. Aβ folds into characteristic beta-pleated sheets

that are highly fibrillogenic and oligomerize to form amyloid plaques (O'Brien & Wong, 2011). Several studies have shown the neurotoxic impact of these aggregates, particularly the longer, hydrophobic forms of Aβ like $A\beta_{1-42}$ (Snyder et al., 1994). $A\beta_{1-42}$ specifically is the most abundant form present in AD brain tissue compared to the control (Selkoe, 1994). Blinded cell transfection experiments found that extracellular $A\beta_{1-42}$ levels increased in *APP, PSEN1,* and *PSEN2* mutant lines, further implicating the peptide in the formation of genetically linked AD (Scheuner et al., 1996). Post-mortem analysis of late-onset AD patients with either a hetero- or homozygous *APOE* mutation also found a significant increase in plaque formation as well as Aβ deposits (Schmechel et al., 1993).

While genetic mutations are a vital element towards potential AD presentation, these genes have been extensively studied through the lens of their influence over plaque quantity – yet research has shown that the severity of the disease doesn't correlate to their abundance (Carter & Lippa, 2005). Clinical observations of individuals with high levels range from normal cognition to diagnosed dementia. This raises a very important question: if Aβ plaque concentration isn't entirely responsible for symptoms, then what other molecular elements contribute to cognitive decline? Before fibrillization and plaque formation, Aβ intermediates undergo several conformational changes like trimer, pentamer, or greater complex forms to create Aβ-derived diffusible ligands – short chains of protofibrils, dodecameric oligomers, and oligomers themselves (Deshpande et al., 2006). In vitro experimentation has shown the neurotoxic impact of Aβ oligomers, other diffusible-ligands, and fibrils

(Deshpande et al., 2006). The oligomers presented the highest level of cytotoxic activity, causing rapid mass neuronal death consistent with initiation of the mitochondrial apoptotic pathway. The diffusible-ligands and fibrils produced similar results, though through increased concentrations on a five-fold longer time frame – suggesting Aβ oligomers may be the leading proponent of neuronal toxicity instead of the convicted fibril plaques (Deshpande et al., 2006). Concurrently, it is plausible to theorize that simultaneous conjunction of all three could result in the loss of neuronal function over time. Further evidence suggests Aβ aggregation may be promoted in the presence of other neurochemicals that chaperone or supervise Aβ self-association, leading to a rise in toxic oligomers easily diffusible across membranes. Clusterin (apolipoprotein J) levels are 40% higher in AD patients, and researchers found that it was able to partially block plaque aggregation while simultaneously forming slow-sedimenting Aβ derivatives. Not only did Clusterin exacerbate the oxidative stress associated with Aβ, but the derivatives themselves comprised readily soluble, non-fibrillar oligomers that were neurotoxic and resistant to dissociation (Oda et al., 1995).

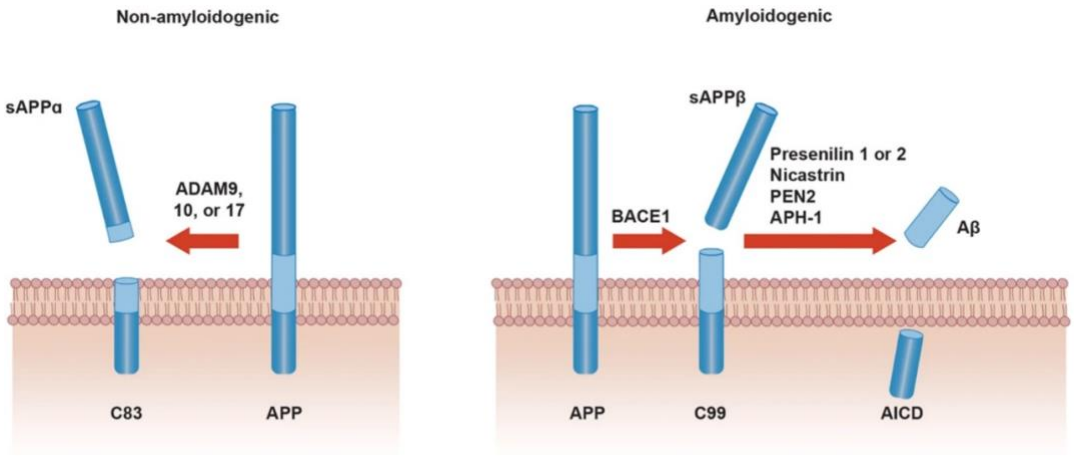

Figure 1: Non-Amyloidogenic vs. Amyloidogenic APP Processing (Hampel et al., 2018).

1.1.1.2 Oxidative Stress

Aside from amyloid-beta proteotoxicity, Alzheimer's patients also present with a rise in oxidative stress and free radicals. As with Aβ, oxidative stress is another prominent potentiator of the disease (Butterfield & Halliwell, 2019). While proteotoxicity has been reported to contribute to this increased stress, it is not the sole causative factor, suggesting oxidation has its own mechanism of action in AD **(Figure 2)**. Oxidative stress is defined as excessive cellular levels of reactive oxygen species (ROS), either through a means of increased production and/or an inefficiency of molecular mechanisms to aid in prompt removal (Cioffi et al., 2019). While reactive oxygen species are naturally occurring, oxidative stress can be counteracted by antioxidant scavenging - however, an imbalance as seen in AD patients can lead to disrupted cellular functionality and molecule formation. For example, interruptions to crucial macromolecules such as the lipoproteins and proteins responsible for

membrane integrity have been observed as a direct response to oxidative stress (Rosa et al., 2018; Wong-Ekkabut et al., 2007). The membranes of cells are comprised of phospholipids, their presence at appropriate ratios is critical for neurotransmission and establishing resting membrane potential and disrupting their makeup can have dangerous consequences. Lipid peroxidation induces a conformational change to the hydrophobic tails, resulting in an extra functional group that bends toward water while the hydrophilic polar heads form hydrogen bonds with water and oxygen – increasing the lipid surface area (Wong-Ekkabut et al., 2007). This change in structural integrity and phospholipid properties reduces membrane bilayer thickness, creating dysfunctional regulation of permeability and potential, otherwise known as leaky membrane. Disruption of the ionic gradients, and thus, membrane potential leads to cell death.

Membrane-associated phospholipids are not the only macromolecules at risk when subjected to high levels of oxidative damage as seen in AD. Due to their abundant, ubiquitous expression and rapid reaction rates, proteins present throughout the body are a prime target for peroxidation (Kehm et al., 2021). Post-translational protein modifications rely on oxidation, lipoxidation, or glycoxidation for proper function in mechanisms like reversible redox reactions – however the nonreversible effects of aberrant oxidative stress are implicated as disease antagonists. This can be seen in patients with mild cognitive impairment (MCI), a condition observed in pre-Alzheimer's individuals. Scientists found increased levels of protein carbonyls, thiobarbituric acid-reactive substances, and malondialdehyde present in patients with

MCI and early-stage AD (Keller et al., 2005). These molecules are a direct result of protein oxidation, where increased concentrations cause a reduction in cognitive memory function, hinting that oxidative stress may be one of the primary points of disease pathology. When considering the aftereffects of these oxidized proteins or membranes, we see an exacerbation in cellular damage through activation of negative metabolic pathways, such as that of p38. A member of the mitogen-activated protein kinase (MAPKs) family, p38 was seen *in vivo* to induce hyperphosphorylated tau in a transgenic Aβ mouse model for *APP/PSEN1* (Giraldo et al., 2014). Aβ-mediated oxidative stress and the resulting tau phosphorylation was prevented with treatment of a p38 inhibitor or vitamin E, leading scientists to conclude that cell signaling plays a pivotal role in disease pathologies and dietary supplementation may be an option for therapies.

1.1.1.3 Bioenergetic Defects

When discussing the impact of oxidative stress, it is important to understand this takes place in a ubiquitous manner. While the plasma membrane and other types of proteins are at risk extracellularly, ROS damage can be found internally - either due to direct stress from inside the cell or through reduced membrane integrity. Specifically, the mitochondria remain susceptible to oxidative stress due to the intrinsic chemical reactions of the electron transport chain (ETC) and its natural production of reactive oxygen species (Chen & Zhong, 2014). AD patients possess

bioenergetic defects and mitochondrial dysfunction in their neurons as a result of Aβ-mediated reduction in key ETC enzymes such as cytochrome c oxidase. In order to combat the natural ROS accumulation from adenosine triphosphate (ATP) production, the mitochondria house an antioxidant enzyme known as Mn-SOD that is downregulated in Alzheimer's animal models. Manganese superoxide dismutase, when inactivated, fails to catabolize ROS; this promotes further bioenergetic dysfunction and even cell death, as verified using an *APP/PSEN1* transgenic mouse (Anantharaman et al., 2006).

Much research points to the mitochondria as another key entry point for disease pathology, which begs the question: what symptom or issue arose first? Based on current research, there is interplay between several pathological factors that exacerbate one another in a positive feedback mechanism **(Figure 2)**. Manzack *et. al* published a paper in 2006 suggesting that the mitochondria may be the initial metaphorical straw to break the camel's back - claiming that it is a direct localization site for Aβ oligomer accumulation, and the resulting oxidative damage emerges from there. Using overexpression mice models for mutant *APP* and Aβ, they found an association between mitochondria and each of the forms – specifically on the inner mitoplast membrane*;* showcasing Aβ may likely localize to mitochondria and cause initial dysfunction (Manczak et al., 2006). They also observed a significant increase in carbonyl proteins, hydrogen peroxide (ROS), and a decrease in cytochrome c oxidase activity prior to Aβ-plaque deposition compared to age-matched controls. All their findings point toward the mitochondria as the initial pathology for AD, leading us to

consider whether targeted mitochondrial therapies could be a future solution or further mitochondria analysis could impart new information about the disease.

Figure 2: Oxidative Stress Model in Alzheimer's Pathology (Chen & Zhong, 2014). The disease pathologies and modalities implicated in Alzheimer's Disease and their impact on other features.

1.1.1.4 Impaired Glucose Metabolism

For the mitochondria to function in its main role as an energy synthesizer, it requires glucose. Glucose metabolism plays an integral role in homeostatic function, with serum blood glucose levels being tightly regulated through absorption, production, uptake, and metabolism pathways. Glucose doesn't act alone, however. Insulin is considered the antithesis of glucose, where activation of the insulin signaling cascade increases muscular and adipose glucose uptake while simultaneously blocking

hepatic sugar production (Saltiel & Kahn, 2001). Insulin not only balances blood glucose concentration – it is also responsible for activating cell growth pathways and lipid formation, as well as glycogen and protein synthesis, among several other vital processes. The delicate balance between glucose metabolism and insulin response is sensitive to metabolic disruptions, where resistance to insulin signaling can occur over long periods of sustained excessive-sugar intake. Insulin resistance (IR) is a key factor of type 2 diabetes and is a major symptom within the neurons of Alzheimer's Disease patients. This symptom causes increased fasting blood sugar levels as desensitization of the insulin receptors prevents uptake and proper metabolism of free glucose (Houstis et al., 2006). Starved of the energy required for proper function, neurons begin to atrophy and die.

Researchers believe that in AD-specific insulin resistance, the presence of amyloid-β aggregates cause neuronal glucose hypometabolism. Several studies have tested this hypothesis, yet always in the context of desensitizing or disrupting the insulin receptor pathway. However, impaired glucose metabolism leads to a change in the glucose transport receptors as well. My research focuses on these integral intramembrane receptors and the impact caused when loss-of-function occurs. Humans have a host of facilitated glucose transporters (GLUTs) that are further characterized into three classes: Class 1, Class 2, and Class 3 transporters (Navale & Paranjape, 2016). Class 1 transporters represent the canonical pathway: those with the highest affinity for d-glucose – the abundant, bioenergetically favorable form of glucose. GLUTs 1-4 encompass this class, where GLUT1 is responsible for basal

glucose uptake due to its ubiquitous expression in all cell types and GLUT3 is predominant in high-energy demand cells such as neurons. GLUT1 is primarily associated with glucose diffusion across the blood-brain barrier where neuron cellular glucose uptake is facilitated by GLUT3. Both GLUT1 and GLUT3 have been implicated in Alzheimer's Disease and possess the highest neuronal expression. Dietary interventions to treat insulin resistance and impaired glucose metabolism involve lowering external sugar consumption through a low-carb or ketogenic diet, in the hopes of repairing desensitization and returning blood-sugar levels to basal concentrations. This therapy decreases activation of the GLUT1 and 3 receptors for energy; instead relying on free L-lactate for ketogenic energy metabolism **(Figure 3)** through MCTs (monocarboxylate transporter) 1 and 2 (Koepsell, 2020).

In our model organism, *Caenorhabditis elegans*, the genes *fgt-1* and *fgt-2* encode for homologs of these GLUT transporters, with the main glucose transporter being *fgt-1* (GLUT3). Loss of *fgt-1* results in improper formation of the vulva due to lack of glucose, presenting in worms with an extruding vulval phenotype (Garde et al., 2022). The ratio of ATP:ADP was lower in *fgt-1* mutants, indicating a defect in proper glucose metabolism. When it comes to *fgt-2* (GLUT1), however, no publications have been made regarding its function.

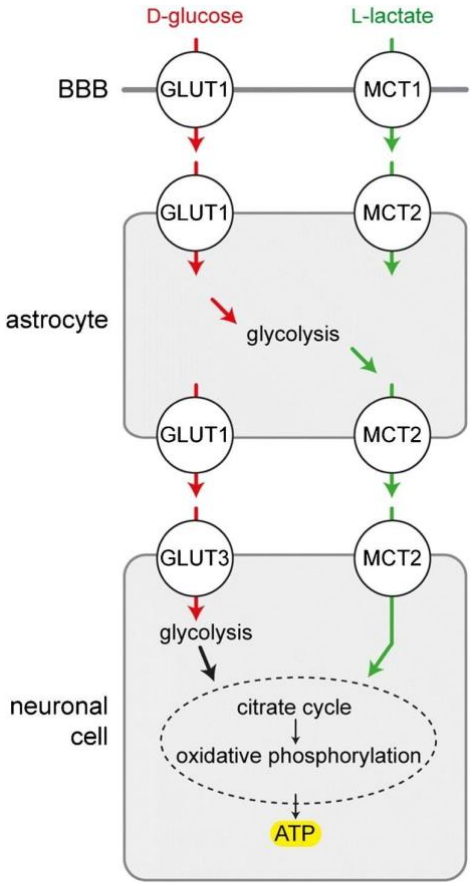

Figure 3: Glucose and Lactate Uptake Pathway (Koepsell, 2020). D-glucose and L-lactate uptake into cells requires activity of GLUT1 and GLUT3 transporters.

1.1.2 Risk Factors

When considering the likelihood of developing a disease, there are factors that can make one individual more at risk than another. Risk factors are broken up into two categories: nonmodifiable and modifiable. Nonmodifiable risk factors are those that cannot be changed, such as age, biological sex, race or ethnicity, and inherited family genetics (Litke et al., 2021). In AD, various inheritable genetic mutations have been

identified and discussed. Females are at higher risk of developing Alzheimer's than men, but the reason remains unclear. Age also plays a significant role in risk ratio, with scientists investigating age-related treatments that focus on delaying natural cellular decay, but these developments are far from being usable in a clinical setting. Modifiable risk factors, however, are those that can be controlled. Exercise, brain acuity games, and diet have been shown to be associated with lower risk of developing AD (Scarmeas et al., 2009). Diet in particular has been extensively studied in recent years, with specific focus on whole-food regimens such as the Mediterranean diet or low-carbohydrate diets like the Ketogenic diet (Ballarini et al., 2021; Grammatikopoulou et al., 2020).

Considering the vital role food plays in our ability to function and thrive, it is of no surprise that what we eat can influence disease progression. Food consists of three major macronutrients – lipids, proteins, and carbohydrates – that are broken down by the body to be used for major metabolism and homeostatic reactions. There are also smaller molecules, micronutrients, which compose of various vitamins and minerals that are typically used as cofactors for important reactions. Combined, macro- and micronutrients keep our bodies running on a daily basis – but how do we know when we've received too little or too much of certain components? As it turns out, it is nearly impossible to accurately gauge the appropriate amount of nutrients required for each person, as genetic influences and gut activity varies per individual. However, general guidelines can be provided for absolute minimum amounts on required nutrients (Institute of Medicine, 2005; Maillot et al., 2010). When

determining which ones can be beneficial or detrimental, however, we run into the issue of personalized genetic interactions as well as overall food complexity. There is no way to control all aspects of dietary intake daily as each item is unique with its own large nutrient profile that can have various other entangled reactions. In addition, the use of single-nutrient vitamins and fixed meal choices still does not eliminate the diversity of every individual's gut microbiome. This is why using simpler models can be a better option for investigating dietary impacts on AD.

1.2 The Role of Diet in Disease

Using diet as a therapeutic intervention is nothing new. The Ketogenic Diet (KD), for example, has been in circulation since the 1920s to treat drug-resistant epilepsy (D'Andrea Meira et al., 2019). Due to the low-carbohydrate nature of this protocol, the Keto diet is said to mimic the effects of starvation or fasting – as the cells switch from glucose abundance to limited glucose levels, the alternative energy pathway that uses fatty acids to power ketone development is activated. Ketones undergo β-oxidation and can be further catabolized into ATP from there. While originally intended for use with epilepsy, the KD has recently gained popularity amongst type 2 diabetes patients – in part due to the decreased body mass, glycolytic load, and fasting blood sugar levels of patients (O'Neill & Raggi, 2020). Every time we eat something with sugar in it, the insulin response pathway turns on in order to return blood sugar levels to basal levels. However, overload of this process can occur over time due to excessive glucose intake. The resulting insulin resistance initiates a

pathological cascade that leads to the presentation and diagnosis of type 2 diabetes (Malone & Hansen, 2019). In this case, we know that what a person consumes can directly cause a disease to manifest and brings to light the potential role diet can play in other conditions onset/progression. Recent focus on neuronal impaired glucose metabolism present in Alzheimer's patients has brought KDs/low-carbohydrate diets into the fold as a potential therapy – and even influenced many within the field to view AD as diabetes type 3. My work will highlight the dietary role/impact glucose transport and metabolism plays on Aβ-proteotoxicity and other AD-like pathologies using the model organism, *C. elegans.*

1.3 *Caenorhabditis elegans* as a Model for AD

C. elegans are small nematodes that eat a simple diet of *E. coli* bacteria. In a lab setting, they are maintained on an NGM (nematode growth medium) agar plate seeded with OP50 *E. coli* and kept at 20℃. These worms are the only known organism with a fully mapped nervous system, making research based around neurodegenerative diseases an enticing target. Within their entire genome, roughly 40% of genes have human orthologs and are highly conserved (Lai et al., 2000; Shaye & Greenwald, 2011). They come in two biological sexes: males (XO) and hermaphrodites (XX). Hermaphrodites possess both a vulva and the male spermatheca and are therefore able to either mate with males or themselves. Due to the nature of hermaphrodite reproduction, genetic experimentation is extremely favorable – as a single worm can provide both the egg and sperm to create a genetic clone. This

affinity for genotype conservation is helpful when experimenting to determine the impact of knockouts, knockins, or CRISPR fluorescent tagging.

In addition to their fully mapped nervous system and level of homology, *C. elegans* have a short life cycle. Wildtype (Bristol N2) animals live on average ~16.7 (Muschiol et al., 2009) to 20 days (Kenyon et al., 1993) from embryo to death under lab conditions. Their short lifespans are accompanied by a large brood size (approximately 290-300 progeny per adult hermaphrodite) that allow for rapid turn around and sample size while conducting studies on age-related diseases such as AD (Muschiol et al., 2009). The nematodes naturally produce the amyloid precursor protein APP; however, they lack the beta secretase enzyme necessary to create the amyloid-beta peptide. Therefore, transgenic animals are required to study this pathology. Our lab uses the AD-model GMC101 (Aβ animals), a transgenic strain that expresses a GFP marker in the intestine and the human $A\beta_{1\text{-}42}$ peptide within the body wall muscles. Upon a temperature upshift to 25℃, Aβ expression and cellular stress leads to a robust visual phenotype, time-dependent paralysis. An example paralysis graph is depicted in **Figure 4**. Using this model, changes in diet may impact the median time-to-paralysis – resulting in a graphical shift either left (acceleration) or right (delay). Expression also induces other AD-like pathological features. Mitochondrial fragmentation, visualized via mito-staining, can be seen in these animals versus wildtype (Lam et al., 2021). This fragmentation is accompanied by a reduction in ATP and an increase in oxidative stress markers like ROS – hallmark features of Alzheimer's Disease patients that are crucial to investigate. Due to the

simplicity of their diet, *C. elegans* are also an ideal candidate for dietary research. Human research revolving around diet is more complex due to the direct and indirect interactions of our gut microbiome (Yilmaz & Walhout, 2014). Worms, however, are a great model to replicate this delicate interplay as they can take in nutrients through the medium and the bacteria **(Figure 5)**.

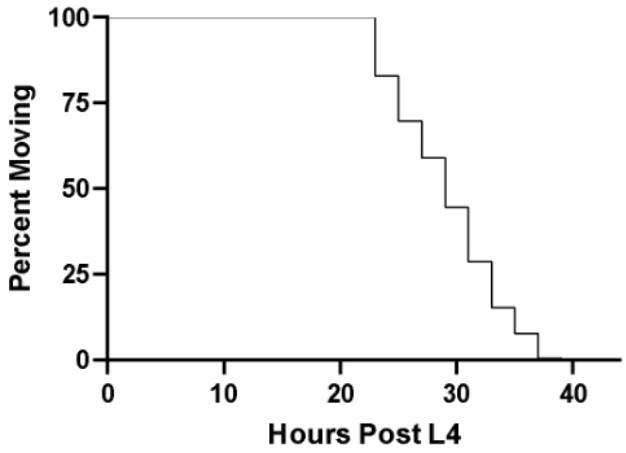

Figure 4: Time-Dependent Paralysis of Aβ Animals. Aβ animals were shifted to 25 degrees C at the end of larval stage 4 (L4).The percent of Aβ-expressing animals moving was recorded every two hours after temperature upshift, starting at 20 hours post-L4.

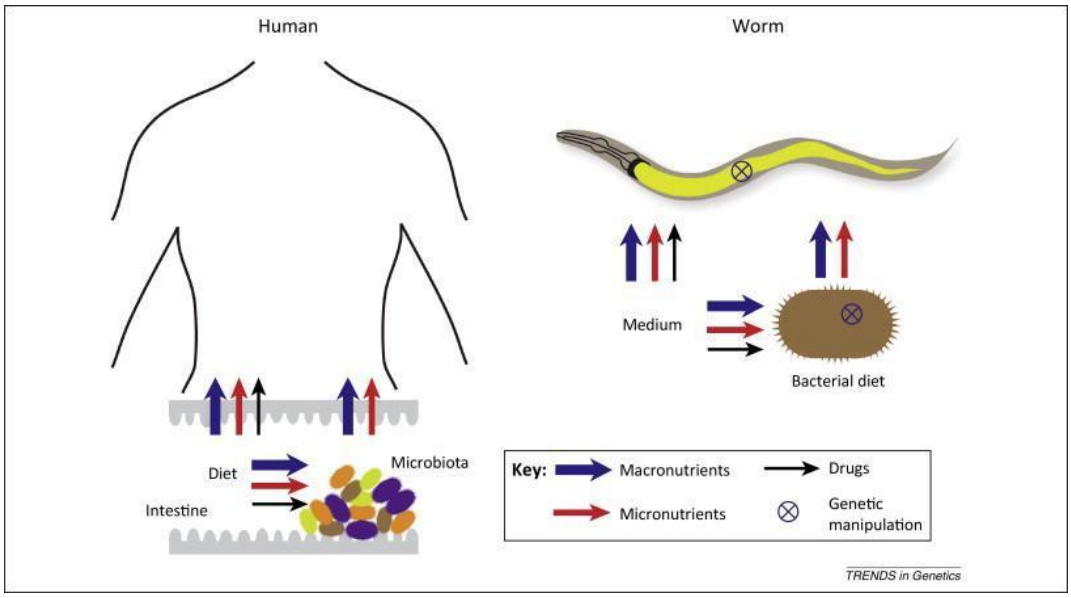

Figure 5: Human versus *C. elegans* Nutrient Absorption (Yilmaz & Walhout, 2014). Translational model of dietary nutrient absorption between humans and *C. elegans*.

1.4 Aims and Hypothesis

Based on previous research within the lab, we hypothesized that a high-glucose diet would have a detrimental impact on AD-like pathological features that could be protected against using dietary and genetic intervention. To test this hypothesis, we first performed paralysis assays using control *E. coli* OP50 and OP50+glucose, as well as vitamin B_{12}-rich *E. coli* HB101 and HB101+glucose supplementation with our Aβ animals. The results of the experiment showed that excessive glucose accelerated Aβ-induced paralysis but the HB101 diet was protective, suggesting the negative effect of a high-sugar diet could be negated with this strain of *E. coli* **(Figure 6)**. Since Aβ expression in *C. elegans* also induces other AD-like pathological features including reduced ATP and increased ROS levels (Lam et al., 2021), we hypothesized that

glucose supplementation would exacerbate reactive oxygen stress and increase overall bioenergetic availability.

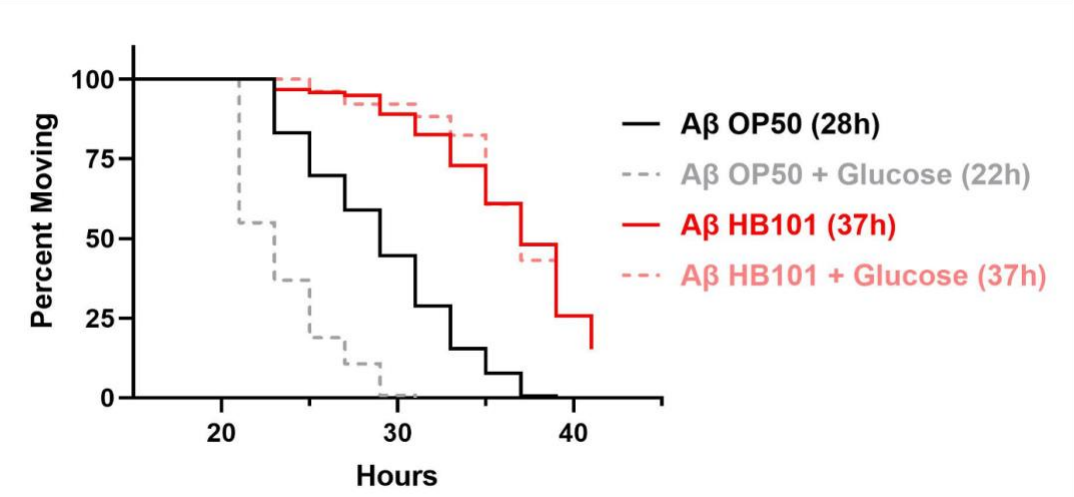

Figure 6: Glucose Supplementation Accelerates Aβ-Induced Paralysis and this is Negated by the HB101 *E. coli* Diet. 10mM glucose supplementation (gray) leads to a dietary shift – an accelerated time-to-paralysis was observed compared to OP50 fed animals (black). HB101 fed animals (red) and glucose supplemented animals (pink) have a delay in time-to-paralysis and removal of the dietary shift. Median paralysis times are shown in parenthesis.

My goal was to determine the impact of glucose toxicity on Aβ-induced proteotoxicity. Using previous literature, I hypothesized that loss-of-function in the GLUT3 and GLUT1 homologs *fgt-1* and *fgt-2* would have protective effects on AD-like features by reducing glucose availability within the cells. To test this hypothesis, I determined how loss of *fgt-1* and *fgt-2* impacted Aβ-induced paralysis, ATP level, ROS accumulation, and glucose uptake.

Chapter 2 METHODS

2.1 Nematode Culture

All *C. elegans* strains used were maintained on 6cm NGM agar plates at 20℃, as described (Brenner, 1974). One liter of nematode growth media is made by combining 2.5g bacto-peptone, 3g NaCl, and 17g agar in distilled water. After autoclaving, media is cooled between 65-70℃ before the following nutrient additives are mixed in: 1 mL cholesterol in ethanol (5 mg/mL), 1 mL 1M CaCl, 1 mL 1M MgSO, and 25 mL 1M potassium phosphate buffer (KH_2PO_4; pH 6.0). Supplementation plates for assays included 10mM or 100mM D(+)-glucose (Fisher Scientific, Cat#: AC410955000 CAS: 50-99-7), 10mM 2-deoxy-glucose (Fisher Scientific, Cat#: L07338.03 CAS: 154-17-6), or 0.1mM methylcobalamin (Millipore Sigma, Cat#: M9756, CAS: 13422-55-4) where indicated. Nutrients were mixed in at 60℃ before being poured. Using a calibrated plate pouring machine, 10mL of media is added into 6cm plates and 25mL into 10cm plates used for ROS and ATP assays. Plates were allowed to dry on the bench for 2 days before being seeded with either OP50, HB101, 10mM glucose, 100mM glucose, or 10mM 2-deoxy-glucose bacterial culture where indicated. NGM plates for maintenance were kept at 4℃ until use. Supplemented plates, both in agar and in culture, were kept at room temperature for no more than 14 days before use.

Gene Identifier	Strain	Allele	Acquired by
Aβ	GMC101	*dvIs100*	CGC
fgt-1	N/a	*tm3165*	National Bioresource Project[1]
fgt-2	N/a	*tm3206*	National Bioresource Project[1]
fgt-1 x fgt-2	UDE246	*tm3165, tm3206*	Genetic cross
Aβ *x fgt-1*	UDE240	*tm3165; dvIs100*	Genetic cross
Aβ *x fgt-2*	UDE218	*tm3206; dvIs100*	Genetic cross
Aβ *x fgt-1, fgt-2*	UDE287	*tm3165, tm3206; dvIs100*	Genetic cross
fgt-2 promoter::mScarlet	UDE257	*henEx22*	construct injection

Table 1: *C. elegans* Mutant Strain Information. *C. elegans* strains generated and used for subsequent experimentation. [1]Tokyo, Japan International *C. elegans* Knockout Consortium (Barstead et al., 2012).

2.2 Bacterial strains

OP50 and HB101 *Escherichia coli* strains were used for experimentation. Bacterial cultures were incubated overnight in LB broth at 37℃ with shaking for approximately 12-16 hours. Supplemental nutrients for glucose and 2-deoxy-glucose cultured plates were added post-inoculation to the concentrations where indicated. Agar plates were seeded with 200µL of bacteria for 6cm and 600µL for 10cm. They were allowed to dry at room temperature for at least 3 days before use.

2.3 Creating Strains

All Aβ strains were created by crossing Aβ males with the deletion mutants. The Aβ transgene (*dvIs100)* was verified via 100% GFP progeny using an AXIO Zoom Microscope. Deletion mutations were verified via standard duplex PCR genotyping (

Table 1). The double mutant UDE246 was created using my spontaneously generated *fgt-2* males. Due to the heat-sensitive nature of the transgene, heat shock for males with any strain containing the Aβ background was impossible. In order to generate my double deletion + transgenic strain UDE287 efficiently, I crossed UDE246 males propagated through heat shock with UDE240, as the genotyping primers for *fgt-2* are stronger and easier to use for PCR detection. I screened for male progeny to confirm a cross and picked 3 GFP^+ L4 F1's onto separate plates to clone. From there I picked 64 GFP^+ F2 progeny onto separate plates and screened for 100% GFP^+ progeny before genotyping for *fgt-1*.

The *fgt-2* promoter::mScarlet strain UDE257 was created by injecting Bristol wildtype worms (N2) with my generated plasmid construct, EAK1. EAK1 consists of the the *fgt-2* promoter inserted at the multiple clone site (MCS) of lab plasmid AES2 using restriction enzymes HindIII and Xbal to drive expression of mScarlet. The plasmid vector also contains the *unc-54* 3' UTR. The construct was injected at 25ng/µL. Worms were co-injected with *rol-6* for the visible roller phenotype. Rollers from the F1 generation were cloned onto plates. 100 F1 roller progenies were screened for stability - the plates with at least 70% rollers were kept for RFP imaging.

2.4 Aβ-induced Paralysis Assay

Animals were synchronized via egg-lay.. 5-6 adult animals were placed onto corresponding supplemented assay plates and allowed to lay eggs for 2-4 hours depending on the number visualized by hour two. The plates were grown at 20℃ and allowed to reach the L4 stage before being shifted to the 25℃ incubator. Depending

on the genotype of the animals, paralysis counts began between 18-36 hours post-temperature upshift. The number of paralyzed versus moving (P:M) worms were denoted every two hours with a total of 2-3 plates per strain each time the assay was performed. Changes between the P:M counts were organized via Microsoft Excel. Median paralysis and probability of survival (percent moving) throughout the experiment were determined using GraphPad Prism software to generate Kaplan Meier survival plots. A log-rank, Mantel-Cox test was used to determine significance in individual experiments. All median paralysis graphs include a minimum of 3 biological replicates. Student's t-test with Welch's correction was used to determine if there were significant differences in median paralysis between genotypes.

2.5 ATP and ROS Quantification

Approximately 1000-2000 age synchronized L1 animals were grown on 10cm plates via bleaching. Assay plates were shifted to 25°C once a majority of animals reached L4 stage and were left in the incubator for 24 hours. The worms were washed off using M9 and collected into 15mL conical tubes before 2000 RPM centrifugation. The M9 buffer was removed from the pellet worms before being washed again with 10mL of M9. This was repeated two more times to ensure no bacteria had been transferred into the tubes. For ATP quantification, Tris-EDTA buffer (100mM Tris, 4mM EDTA pH 7.75) was used for the last wash step. Final removal of the buffer to ~200µL was performed before using glass pasteur pipettes to transfer the worm pellets to sterile 1.5mL microcentrifuge tubes. Samples were flash frozen with dry ice once before being thawed for sonication. After being sonicated on ice for 4 minutes, samples were centrifuged at 14,000 RPM for 10 minutes at 4°C. The supernatants were collected and transferred to sterile 1.5mL microcentrifuge tubes before

experimentation. ATP quantification was performed using the ATP Bioluminescence Assay Kit CLS II (Roche Diagnostics, Cat#: 11699695001) and fluorescence was detected by the Glomax Multi-Detection System reader. Levels were then normalized to 25µg protein content identified via the Pierce BCA protein kit (ThermoFisher Scientific, Cat#: 23327). Each sample was performed in triplicate, and due to instrumentation issues, only received two biological replicates per condition.

The animal lysate preparation for ROS quantification was identical to the ATP assay, aside from the Tris buffer - M9 was substituted. Samples were still normalized to 25µg of protein. Hydrogen peroxide (H_2O_2) levels were measured using 2′,7′-Dichlorofluorescein diacetate/H2DCFDA (Sigma-Aldrich, Cat#: D6883-250, CAS: 4091-99-0) incubated with the samples for six hours on a 96-well black plate. H2DCFDA binds to hydrogen peroxide and fluoresces upon excitation, allowing for detection using the Glomax Multi-Detection System. As with the ATP assay, each sample was performed in triplicate for technical precision and accuracy. A minimum of 3 biological replicates were used for each dietary condition and strain.

2.6 Glucose Quantitation Assay

Total Body Glucose Quantitation was performed using the same animal lysate preparation as indicated above. Using the Amplex™ Red Glucose/Glucose Oxidase Assay Kit (Invitrogen, Cat#: A22189), I measured whole body glucose due to the reaction between glucose oxidase with d-glucose to create d-gluconolactone and hydrogen peroxide. The Amplex™ Red reagent, in conjunction with horseradish peroxidase (HRP), reacts with H_2O_2 and emits a red fluorescent resorufin at a 1:1 ratio. Samples were diluted five-fold using the pH-controlled 1x reaction buffer. A glucose standard curve was prepared per manufacture instruction. Fluorescence was measured

using a Glomax Multi-Detection Plate Reader after 30 minutes. Protein concentration was used to normalize samples to 25µg via Pierce BCA protein kit. Each sample was performed in triplicate with a total of 2 replicates.

Chapter 3 RESULTS

3.1 Analysis of Aβ Supplemented with High Dietary Glucose and Vitamin B_{12}

The *C. elegans* Alzheimer's strain, GMC101, expresses the toxic human $A\beta_{1-42}$ peptide in their body wall muscles upon a temperature upshift to 25°C. This results in a robust time-dependent paralysis that is easy to visualize and quantitate. Varying assay conditions, specifically dietary supplementation, can have a profound impact on the time-to-paralysis, as well as other AD-like pathological features like reactive oxygen species and bioenergetic availability. A previous Ph.D. student, Dr. Andy Lam, showed in his 2021 paper that the *E. coli* strain HB101 was able to induce a shift right in time to paralysis compared to standard lab *E. coli* OP50 (Lam et al., 2021). He also showed that HB101 was able to abrogate the shift-left, or accelerated time-to-paralysis, caused by glucose toxicity. We were curious to see if this phenomenon was caused by vitamin B_{12}, as HB101 is a vitamin B_{12}-rich strain.

To determine if vitamin B_{12} was the nutrient within HB101 providing protection against glucose toxicity's acceleration, we performed paralysis assays using vitamin B_{12} and glucose supplemented plates. Vitamin B_{12} did provide slight protection and induced a dietary-shift right – as seen in **Figure 7**. Animals on B_{12}+10mM Glucose OP50 (green solid) paralyzed at 28 hours post-shift while those grown on 10mM Glucose OP50 (red solid) had a median paralysis of 24 hours.

However, the detriment of glucose isn't completely removed by just B_{12} supplementation when also factoring in the B_{12} OP50 (black solid) with a median time-to-paralysis of 36 hours. The 10mM Glucose HB101 (red dashed) and vitamin B_{12}+10mM Glucose HB101 (greed dashed) both had a median of 40 hours, suggesting that there is another element or nutrient within HB101 *E. coli* that is providing protection other than B_{12}.

While inducing expression of Aβ causes this visible paralysis phenotype, it also presents with other AD-like pathogenic features on a molecular level. To determine whether vitamin B_{12} had an impact on reactive oxygen species, I performed a hydrogen peroxide assay to quantitate the accumulation of ROS between different conditions. Dr. Lam had previously shown in his paper that vitamin B_{12} will restore ROS levels to wildtype when supplemented. I was able to reproduce these results (*$p<0.05$) and show that the near three-fold increase in H_2O_2 caused by glucose toxicity can be negated (****$p<0.0001$) through B_{12} supplementation **(Figure 8)**. These results indicate one potential reason why B_{12} provided a slight protection in time-to-paralysis.

Surprisingly, the addition of 10mM glucose had no impact on ATP levels in Aβ animals **(Figure 9)**. Due to the nature of bioenergetic creation and its need for readily available glucose to function, it was interesting to see that additional glucose didn't equate to additional energy synthesized. Overall, Aβ animals on either control or 10mM glucose had lower ATP compared to wildtype (data not shown). Unfortunately, I was unable to perform this experiment again using vitamin B_{12} due to failure of the injection system in the Glomax plate reader.

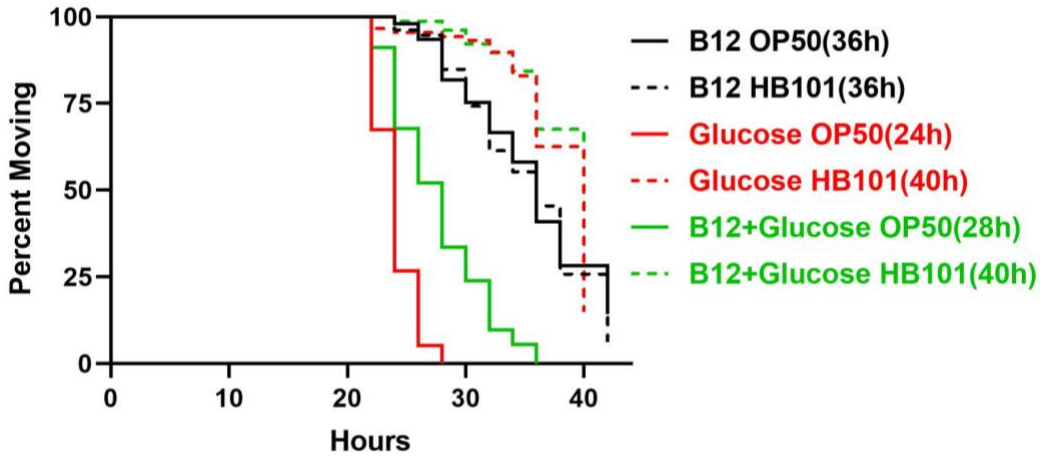

Figure 7: Vitamin B_{12} Provides Some Protection Against High Dietary Glucose Accelerated Time-To-Paralysis in Aβ animals. Aβ worms grown on agar plates supplemented with either B_{12}, 10mM Glucose, or B_{12}+10mM Glucose and seeded with one of two *E. coli* bacterial cultures: OP50 (solid lines) or HB101 (dashed lines). Median paralysis times are shown in parentheses.

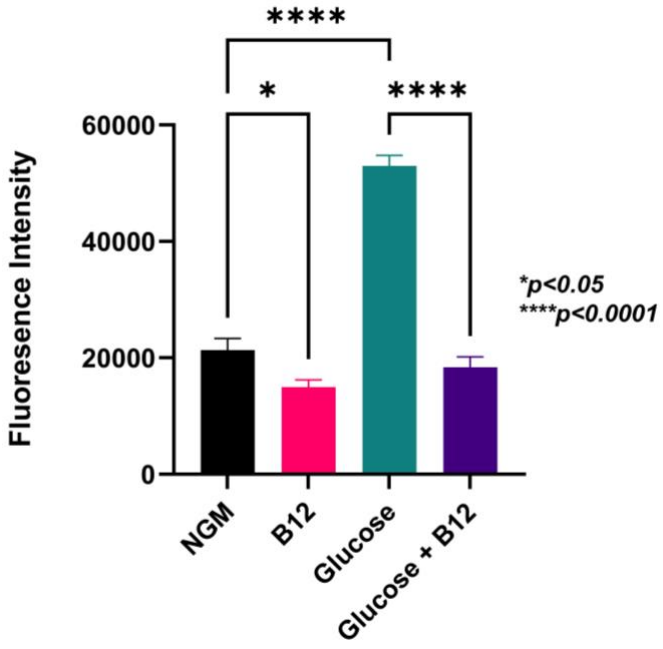

Figure 8: Vitamin B_{12} Protects Against ROS Accumulation from High Dietary Glucose. Aβ worms grown on agar plates supplemented with either vitamin B_{12}, 10mM glucose, or both; all plates were seeded with OP50 *E. coli*

bacterial culture. Vitamin B_{12} (pink) caused a significant decrease in H_2O_2 accumulation (*p<0.05), while 10mM glucose (teal) led to a significant increase (****p<0.0001) that was significantly reduced when plates were supplemented with vitamin B_{12} (purple). n<4

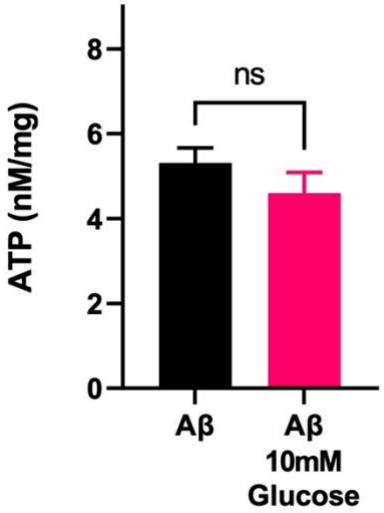

Figure 9: High Dietary Glucose Has No Impact on ATP Levels. Aβ animals grown on either NGM (black) or 10mM glucose (pink) agar plates. ns=not significant, n=3.

To investigate gene expression changes occurring due to differences between the two *E. coli* strains, I analyzed RNAseq data generated by previous Tanis lab graduate student Kirsten Kervin. The facilitated glucose transporter, *fgt-2*, was one of several genes upregulated in OP50 fed animals compared to those on HB101 **(Figure 10)**. This suggested that glucose transport may play a role Aβ-induced paralysis. We ordered the *fgt-2* knockout strain from the Tokyo Japanese Knockout Consortium for further experimentation.

Gene	Predicted Function	logFC
fgt-2	glucose transporter	2.04
acdh-1	acyl-CoA dehydrogenase	4.19
fat-7	fatty acid desaturase	2.79
folt-2	folate transporter	2.36
C45E5.1	phosphoglycolate phosphatase	1.61

Figure 10: Differentially Expressed Genes in Aβ animals Fed Different Diets. A subset of the RNAseq data showcasing significantly upregulated genes in OP50 fed Aβ animals compared to HB101.

3.2 Analysis of *fgt-2* Mutants Expressing Aβ, Supplemented with High Dietary Glucose and Vitamin B_{12}

In *C. elegans*, Garde *et al.* showcased in 2021 that the gene *F14E5.1* was part of the solute-carrying family of transporters for glucose (Garde et al., 2022). The gene was subsequently renamed *fgt-2 (*also known as *fdgt-2)*. Since *fgt-2* was downregulated in HB101 fed animals, we expected to see protection through impaired function. To investigate the impact loss of *fgt-2* causes in Aβ-induced pathologies, I crossed the *fgt-2* allele deletion *tm3206* with the Aβ transgene *dvIs100*

To begin, I performed the paralysis assay using control Aβ animals versus Aβ*; fgt-2* knockout animals fed either OP50 or HB101 *E. coli.* Loss of *fgt-2* removed the dietary shift typically seen between the two bacterial strains, and overall provided a significant delay in the median time-to-paralysis **(Figure 11)**. Mutant animals fed OP50 (blue solid) exhibited paralysis in line with control animals fed HB101 (grey dashed) and had no significant difference against mutants fed HB101 (blue dashed).

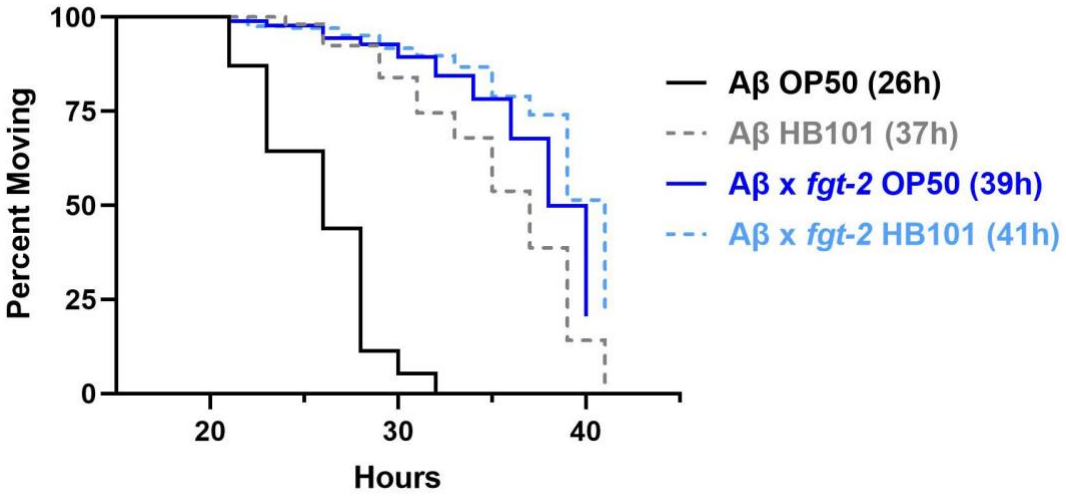

Figure 11: Loss of *fgt-2* Delays Aβ-induced Time-to-Paralysis. Aβ animals fed HB101 (grey dashed) exhibit a significant dietary shift compared to Aβ animals fed OP50 (black solid). Loss of *fgt-2* removes the shift between the two diets; OP50 fed mutants (blue solid) and HB101 fed mutants (blue dashed) median time to Aβ-induced paralysis are comparable to the HB101 control (grey dashed).

Repeating the paralysis assay with the addition of 10mM glucose saw interesting results. Mutants grown on either OP50 (blue solid) or OP50+10mM glucose (blue dashed) acted almost identical, with median times-to-paralysis at 39 hours and 38 hours, respectively **(Figure 12)**. They were also on par with the control HB101+10mM glucose (red solid) with a median time of 37 hours. The loss of *fgt-2* was able to remove the shift seen between glucose supplementation on OP50 **(Figure 13)** and between the two bacterial strains **(Figure 14b)**, however, failed to eliminate the shift between OP50+10mM glucose and HB101+10mM glucose **(Figure 14a)**. This can be seen in **Figure 12** when comparing mutant OP50+10mM glucose (blue dashed) and HB101+10mM glucose (green solid). It is important to note that while the representative experiment shown exhibits control animals fed HB101+10mM glucose

(red solid) as significant against the mutants (green solid), the average median time-to-paralysis for 3 biological replicates is not significant **(Figure 14a)**.

These results suggest that loss of *fgt-2* is one key pathway necessary for general protection through HB101 *E. coli*; however, when factoring in the addition of glucose it is clear another element within HB101 must be providing additional protection against toxicity. When comparing the data obtained for OP50 and OP50+10mM glucose, one can infer that *fgt-2* plays a pivotal role in the progression of glucose toxicity – potentially by modulating the import and/or export of sugar and thus impacting the downstream effects of glucose metabolism. The differential impact between the two strains poses more unanswered questions to be discussed for future experimentation.

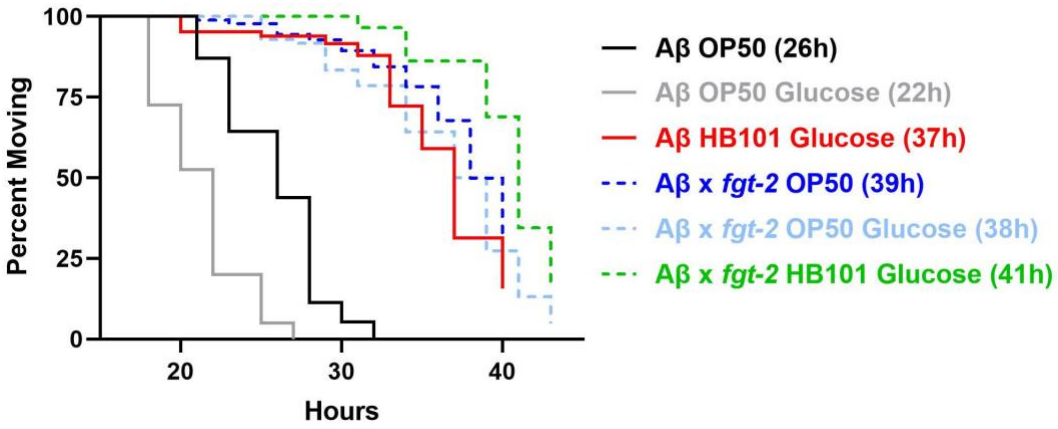

Figure 12: Loss of *fgt-2* Eliminates the Detrimental Impact of Glucose on Aβ-Induced Paralysis. Mutant animals grown on OP50+10mM glucose (blue dashed) exhibit elimination of the dietary shift caused by excessive glucose when compared to OP50 mutant animals (blue dashed). On average, HB101+10mM glucose mutants (green dashed) showed a slight delay in median paralysis when compared to the OP50+10mM glucose mutants (blue dashed), but not HB101+10mM glucose control animals (red solid).

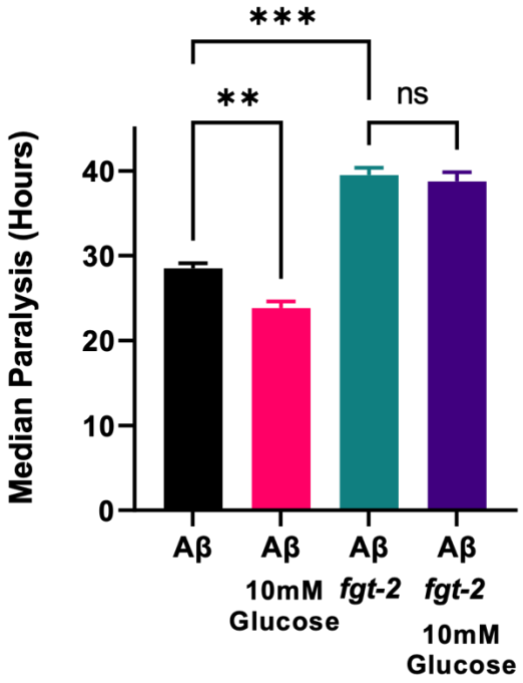

Figure 13: Loss of *fgt-2* Removes the Dietary Shift caused by Glucose. *fgt-2* mutant animals fed the OP50 *E. coli* food source with 10mM glucose (teal) have a median time-to-paralysis similar to those grown without glucose supplementation (purple). Control Aβ animals grown on NGM (black) exhibit a significant earlier time-to-paralysis (***$p<0.0005$) compared to mutants (teal). Control animals grown on 10mM glucose (pink) exhibit acceleration (**$p<0.005$) compared to control grown on NGM (black). $n<3$.

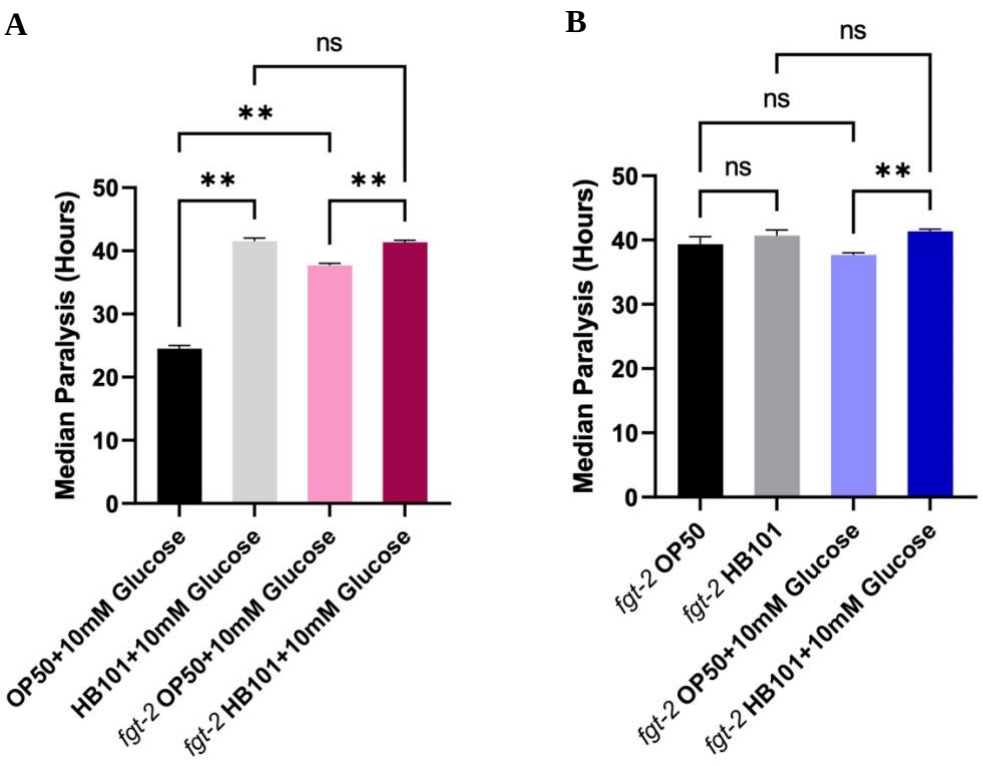

Figure 14: Control versus *fgt-2* Mutant Median Time to Aβ-Induced Paralysis. **(A)** Median time-to-paralysis for control and mutant animals grown on 10mM glucose plates seeded with either OP50 or HB101. Control animals exhibit a dietary shift (**p<0.005) between the two *E. coli* strains. Loss of *fgt-2*, while overall delaying the time-to-paralysis (**p<0.005) compared to control, fails to completely remove the dietary shift between OP50 and HB101 when supplemented with 10mM glucose. Control and mutant worms fed HB101+10mM glucose have no significant change in time-to-paralysis; n≥3. **(B)** Comparison of median time-to-paralysis for the *fgt-2* mutant in all conditions. Loss of *fgt-2* removes the dietary shift between OP50 and HB101 but fails to remove this when excess glucose is present (**p<0.005); n≥3.

To determine the impact loss of *fgt-2* had on reactive oxygen species and energy synthesis, I performed the H_2O_2 and ATP quantitation assays again with my mutants. Knockdown of *fgt-2* (purple) abrogated the near three-fold ROS increase (****p<0.0001) seen in control animals (pink) when grown on OP50+10mM glucose

(Figure 15a). When considering the previous data, one can hypothesize that this decrease in oxidative stress may be one contributing factor in the delayed time-to-paralysis. The results from ATP quantitation may further attribute to this aspect, as the loss of *fgt-2* significantly increased free-energy (*p<0.05) **(Figure 15b)**. It is important to note that these results consist of animals grown on agar plates seeded with OP50. Further experimentation is needed to identify the impact HB101 has on these metrics in comparison to OP50.

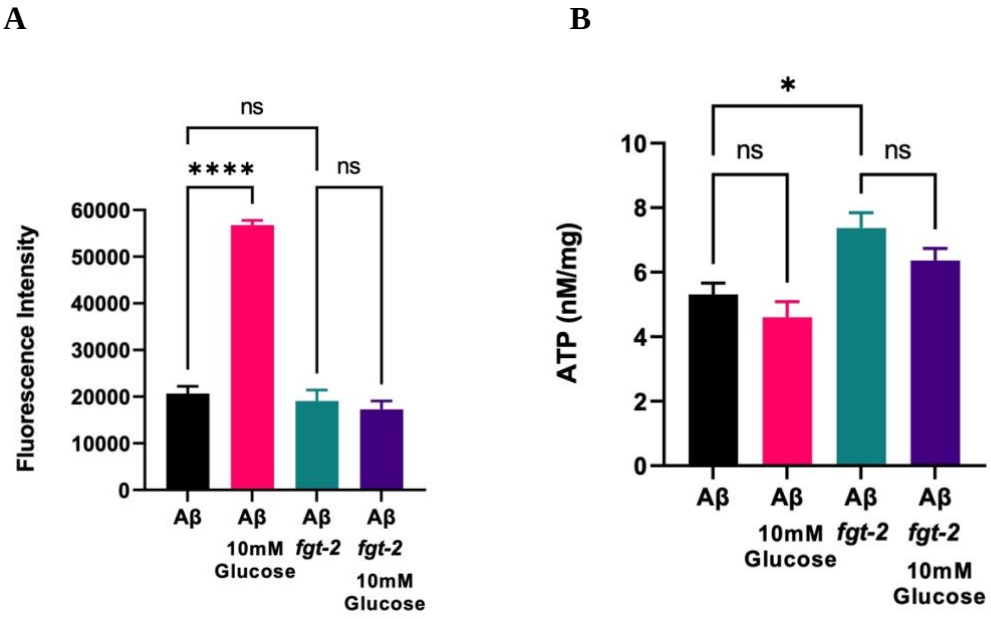

Figure 15: Loss of *fgt-2* Impacts ROS Accumulation and ATP Levels. (A) Hydrogen peroxide levels in control and *fgt-2* mutants (+/-) 10mM glucose. Control Aβ animals supplemented with 10mM glucose show significantly higher (****p<0.0001) ROS accumulation versus Aβ and Aβ; *fgt-2* mutant animals grown without glucose supplementation. Glucose did not impact ROS accumulation in *fgt-2* mutants; n≥3. **(B)** ATP levels in Aβ and Aβ; *fgt-2* mutants (+/-) 10mM glucose. Glucose had no impact on ATP in Aβ worms. *fgt-2* mutant ATP levels were significantly higher (*p<0.05) than the control; supplementing with glucose had no effect. n=2.

Interestingly, when repeating these experiments utilizing vitamin B_{12}, I saw a detrimental impact on ROS and ATP levels. Mutant animals grown on OP50+148 nM B_{12} showcased a significant increase in hydrogen peroxide levels (*$p<0.05$) compared to the OP50 control **(Figure 16a)**. The addition of 10mM glucose further exacerbated accumulation when compared against B_{12} (**$p<0.005$) and control (*$p<0.05$). These results are strengthened further by the outcome of the ATP quantitation **(Figure 16b)**. Regardless of glucose supplementation, animals grown with vitamin B_{12} have significantly lower (*$p<0.05$) free energy. This raises several questions regarding the antithetic impact vitamin B_{12} has on control versus *fgt-2* mutants and how they relate or contribute to the median time-to-paralysis.

Because *fgt-2* had not been studied before, I wanted to investigate its spatiotemporal expression pattern. Obtaining this information required the creation of a fluorescently tagged plasmid construct. We injected this *fgt-2* promoter::mScarlet construct, isolated animals with stable extrachromosomal arrays, and then imaged these animals using the Andor Dragonfly Confocal Microscope.

Upon observation, I was able to confirm that *fgt-2* is expressed in several cell types, including the body-wall muscles, intestine, neurons **(Figure 17 and Figure 18)**, and pharyngeal muscle (data not shown). Because this strain was made using an extrachromosomal array, the animals display mosaicism in the RFP expression pattern. This is also using a transcriptional reporter, and a translational reporter would have to be used to determine where the protein localizes. However, this gives a general idea of when the RNA transcript is being made and in which cell type.

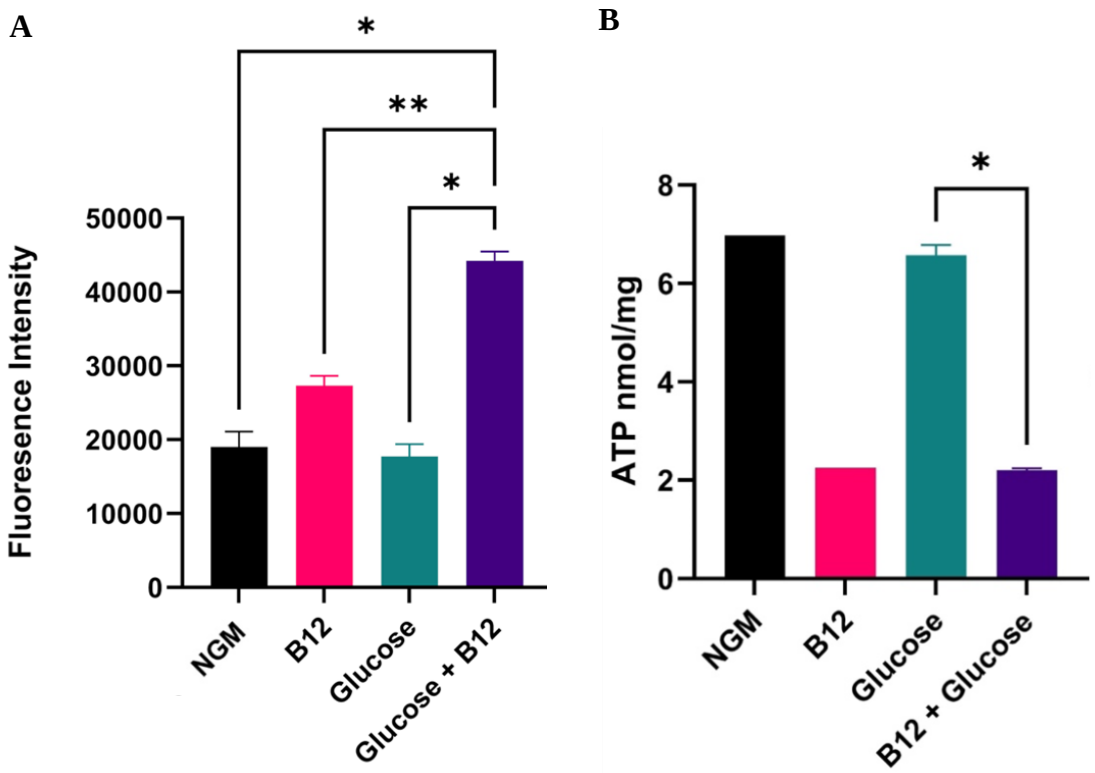

Figure 16: B_{12} Supplementation of *fgt-2* Mutants Negatively Impacts ROS and ATP Levels. (A) Hydrogen peroxide levels in *fgt-2* mutants exposed to various supplementation conditions. B_{12} supplementation resulted in a significant (*$p<0.05$) increase in H_2O_2 when paired with 10mM glucose. No significance was seen between control and 10mM glucose. n=2. **(B)** Graph shows the comparison of ATP levels in *fgt-2* mutants grown on various supplementation plates. Animals grown on B_{12} + 10mM glucose saw a significant decrease (*$p<0.05$) in ATP compared to the 10mM glucose. Not enough trials were performed to determine significance for NGM and B_{12} plates.

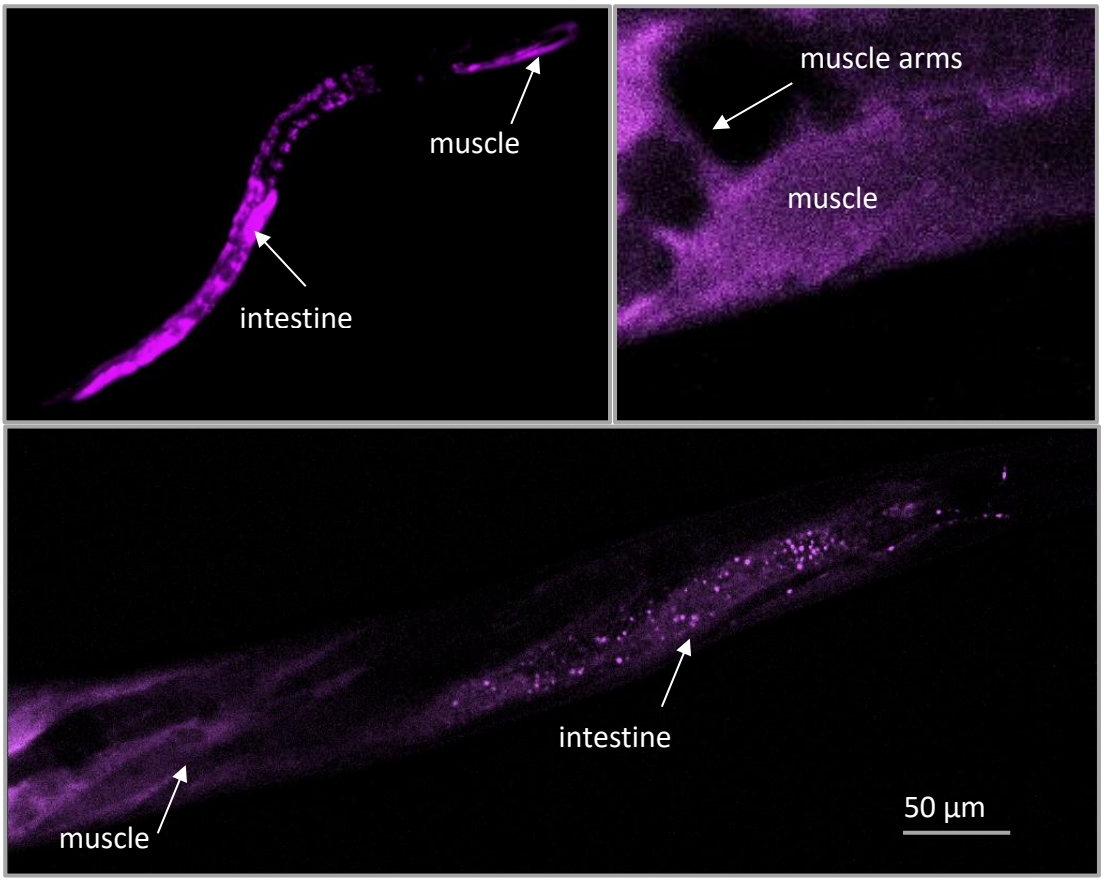

Figure 17: A *fgt-2* Transcriptional Reporter Reveals Intestinal and Muscular Expression. Images captured using L4 and adult worms paralyzed using levamisole and staged on agarose pads. ImageJ was used for analysis and color-blind recoloring. Scale, 50 µm.

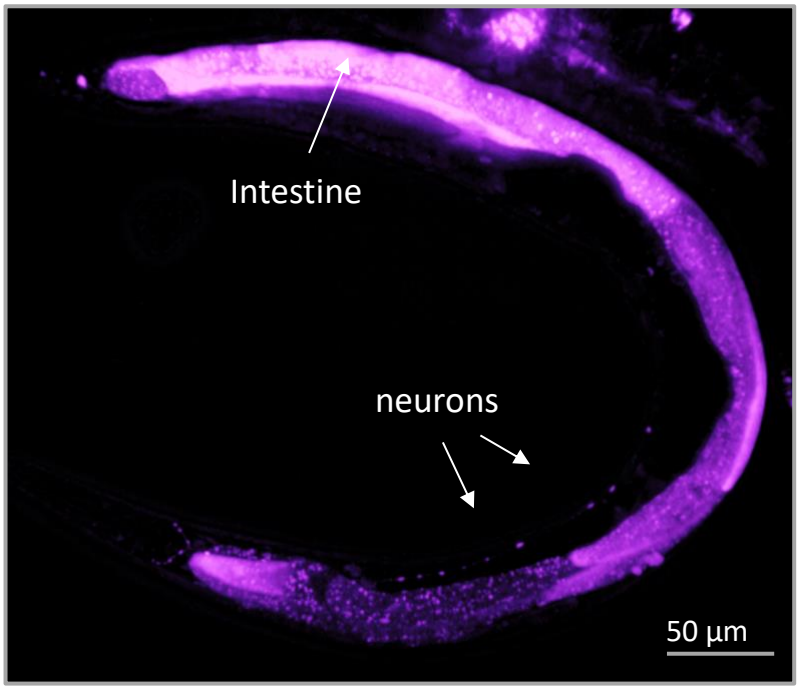

Figure 18: A *fgt-2* Transcriptional Reporter Reveals Neuronal Expression. Images captured using L4 and adult worms paralyzed using levamisole and staged on agarose pads. ImageJ used for analysis and color-blind recoloring. Scale, 50 µm.

3.3 Analysis of Aβ; *fgt-1* and Aβ; *fgt-1*;*fgt-2* Animals Supplemented with High Dietary Glucose

As previously mentioned, the primary glucose transporter in *C. elegans* is *fgt-1* (also known as *fdgt-1*). While *fgt-2* seems to play a role in glucose metabolism, it is not the main transporter responsible for allowing sugar into or out of the cell. I was interested in determining the impact loss of *fgt-1* would have in comparison to *fgt-2* so I crossed the *fgt-1* knockout allele *tm3165* with Aβ. Loss of *fgt-1* had a detrimental impact on the rate of paralysis. Mutant animals fed OP50 (teal) had an accelerated time-to-paralysis in comparison to the control (black) (*$p<0.05$) **(Figure 19)**. The addition of 10mM glucose (purple) saw no significant change in median paralysis, indicating loss of *fgt-1* removes the dietary shift typically seen when excess glucose is

present – albeit detrimental overall compared to control **(Figure 19)**. This suggests that while glucose transport into/out of the cell is important for combating proteotoxicity, excessive glucose should still be avoided.

As shown in **Figure 20** and **Figure 21**, loss of *fgt-1* removed the dietary shift present between OP50 and HB101 *E. coli*. *fgt-1* mutants grown on HB101 (red) have a similar time-to-paralysis as those on OP50 (black) and OP50 + 10mM glucose (dashed grey), however are significantly accelerated compared to HB101 + glucose (dashed red) **(Figure 20)**. On average, *fgt-1* animals fed OP50 have a median paralysis of 23 hours, OP50 + glucose at 24 hours, HB101 with 27 hours, and HB101 + glucose at 38 hours **(Figure 21)**. Glucose-only conditions for both the control and *fgt-1* can be better visualized in **Figure 22b.** This suggests that loss of *fgt-1* removes the protection HB101 provides against Aβ-induced proteotoxicity and can be restored through the addition of glucose. It is possible that there is a secondary pathway being activated when glucose is supplemented and allows it to behave as a positive cofactor to restore protection. When reconsidering *fgt-2*, we can further identify differences between the two transporter genes and their impact on paralysis.

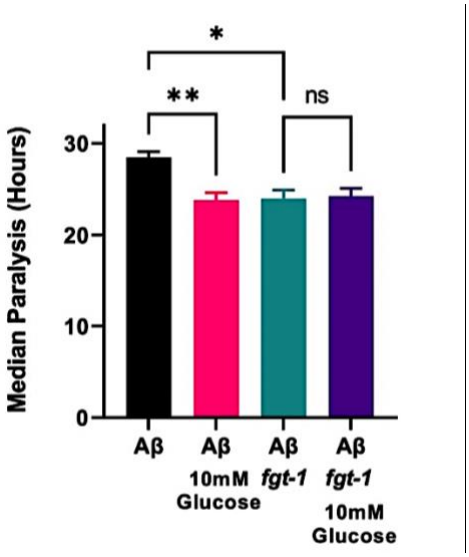

Figure 19: Impact of loss of *fgt-1* on Median Paralysis in Aβ Animals Fed OP50. Median time-to-paralysis of control Aβ animals versus Aβ; *fgt-1* mutants (+/-) 10mM glucose. Loss of *fgt-1* causes a significant acceleration (*p<0.05) in time-to-paralysis compared to the control. Control animals fed 10mM glucose exhibit a significant decrease in median paralysis (**p<0.005) compared to control but see no significant difference from *fgt-1* mutants. n≥3.

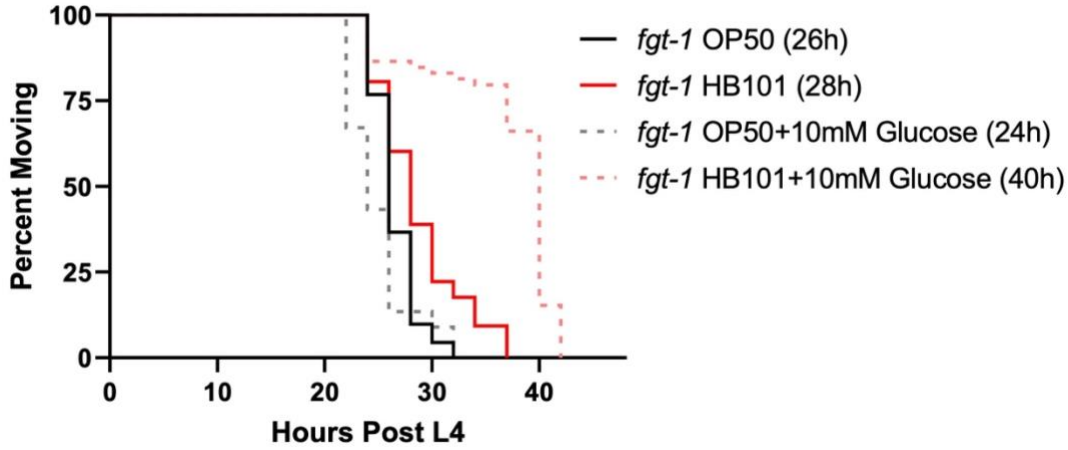

Figure 20: Loss of *fgt*-1 Eliminates the Dietary Shift Caused by the OP50 and HB101 *E. coli* Diets. *fgt-1* mutant animals fed OP50 *E. coli* (black) present with a similar time-to-paralysis as HB101 (red). HB101 is accelerated compared to previous data and is restored when animals are supplemented with glucose (dashed red).

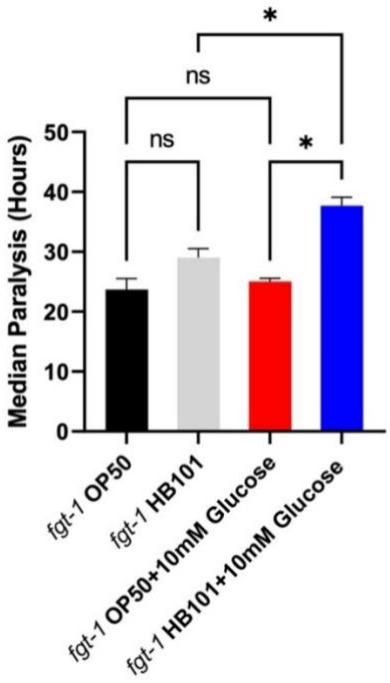

Figure 21: Loss of *fgt-1* Negates the Beneficial Impact of the HB101 Diet. The dietary shift in Aβ-induced paralysis seen when the control Aβ strain is fed the two different strains of *E. coli* is not observed in the *fgt-1* mutant. Addition of 10mM glucose to agar plates seeded with HB101 bacteria restores the protective impact against proteotoxicity in the *fgt-1* mutant (*p<0.05). n=3.

Comparing the results between the two mutant strains supplemented with glucose reveals a failure to remove the shift induced by toxicity. In the case of *fgt-2,* while knockout of the gene was beneficial, HB101 *E. coli* still caused a slight delay in time-to-paralysis compared to OP50 on glucose supplemented plates **(Figure 22a)**. Similarly, loss of *fgt-1* caused a shift between OP50 and HB101 – where the addition of glucose was beneficial instead of detrimental. Because there is no significant difference between *fgt-2* fed OP50 + glucose and *fgt-1* fed HB101 + glucose, several questions arise regarding how interlinked the two transporters are and whether they

can play compensatory roles when experiencing loss of function as hypothesized previously (Garde et al., 2022).

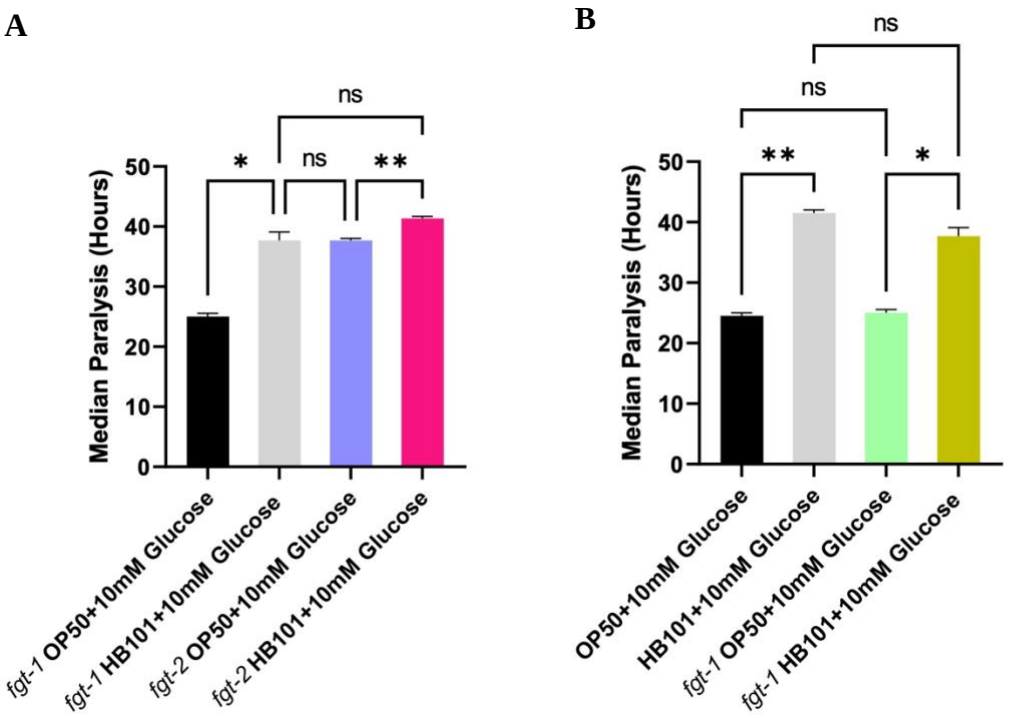

Figure 22: Loss of *fgt-1* Fails to Remove Glucose-Induced Dietary Shift in Aβ-Induced Paralysis. (A) Median time-to-paralysis for *fgt-1* and *fgt-2* mutants fed different diets and supplemented with 10mM glucose. Loss of *fgt-1* fails to remove the dietary shift between the strains (*p<0.05). HB101 fed *fgt-1* mutants perform similar to OP50 fed *fgt-2* mutants, while *fgt-2* mutants exhibit a small, but significant difference when fed the two different bacterial diets (**p<0.005). n=3. **(B)** Comparison of median time-to-paralysis between control animals and *fgt-1* mutants on glucose. Control animals perform similar to *fgt-1* mutants on OP50 and see a dietary shift when fed HB101 *E. coli* (**p<0.005) n=3.

Based on the results above, I was interested in looking at the effect loss of both transporters would have on paralysis. Because the knockout of *fgt-2* is beneficial and loss of *fgt-1* is detrimental, I wondered if there would be a dominant phenotype or a mix of the two. Does *fgt-2* rely on functional *fgt-1* to provide protection? Is the loss of

the primary transporter too great to overcome or do they involve completely different pathways? In order to observe the impact this causes I created a double mutant with the Aβ transgene. Completing the paralysis assay revealed that the *fgt-1; fgt-2* double mutant (purple) performs in a manner similar to the *fgt-1* single mutant (pink) **(Figure 23)**. While this suggested *fgt-1* was necessary for the protection *fgt-2* provides, more experimentation is necessary using HB101 to observe and investigate this further.

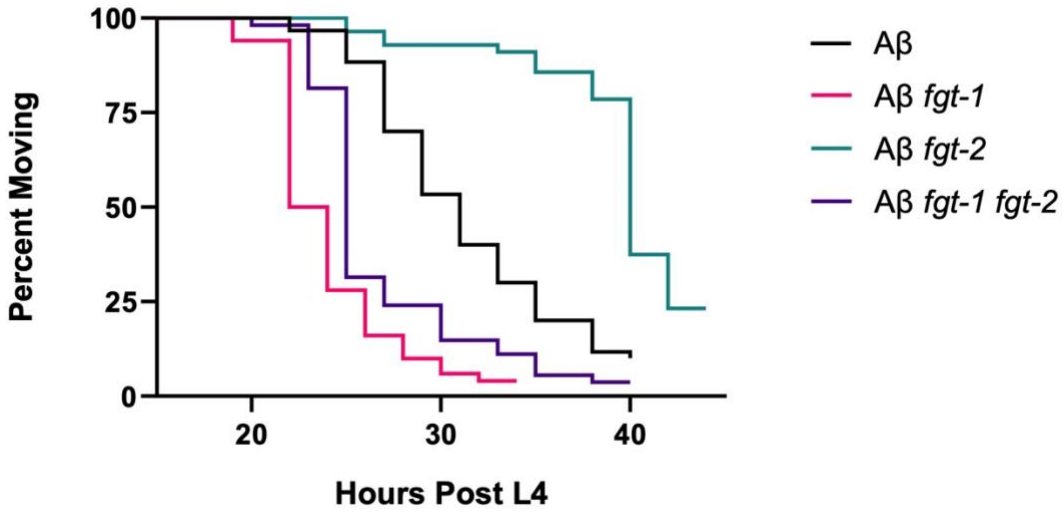

Figure 23: The *fgt-1*; *fgt-2* Double Mutant Exhibits Aβ-Induced Paralysis Similar to that Observed in the *fgt-1* Mutant. Loss of both glucose transporters presents with the *fgt-1* phenotype; double mutants (purple) paralyzed similar to *fgt-1* mutants (pink).

Because *C. elegans*, like humans, can receive nutrients either through the medium or bacteria, I wanted to make sure that the animals were metabolizing the supplemented glucose, and by that effect, was the reason for these effects. It is important to remember that *E. coli* is a living organism with their own metabolic system and it is possible their reaction products – not the glucose specifically – is causing these changes. To test this, I used a non-metabolizing form of glucose, 2-

deoxy-glucose (2-DG), as a supplemental nutrient. I also added the nutrients directly into the culture, to see if this had a different impact than when it was added to the agar plates before pouring. Upon conducting this experiment, I observed a removal of the dietary shift between OP50 (black) and OP50 + 10mM glucose (blue) **(Figure 24)**. They had a median paralysis of 31 hours and 30 hours, respectively, and it is possible that the bacteria used up all the glucose in solution before the worms were able to have access. However, 100mM glucose in the *E. coli* culture medium led to results similar to 10mM glucose supplemented in agar. It is plausible that the 10-fold increase in concentration provided more sugar than was able to be metabolized in the growth period for *E. coli* – therefore allowing the nematodes to ingest the macronutrient as they had when it was present in the agar.

This assay also showed that in order for glucose to have an effect, it must be metabolized. The 2-DG animals (green) had no significant difference in median time-to-paralysis compared to the control or 10mM glucose. Without interference of *E. coli* metabolism, supplementation of 2-DG at 10mM would either induce a shift – if due to glucose accumulation - or not – if due to worm metabolism. The results shown indicate that the sugar must be metabolized to have an impact. For me to confirm this concept, I completed a preliminary total body glucose assay to measure the glucose levels as seen in **Figure 25** to be discussed more below. Analysis of total glucose in animals fed OP50 without glucose supplementation showed a significant difference (*$p<0.05$) between my *fgt-1* and *fgt-2* mutants (**Figure 25a)**. Interestingly, there was no significant change between no supplementation and 100mM glucose supplementation for all strains **(Figure 25b).** This suggests that they could either be metabolizing the excess glucose immediately or didn't consume it. However, the latter

point would be unlikely considering the paralysis shift in **Figure 24**. I will need to conduct the glucose uptake experiment in order to determine whether uptake is changing with supplementation.

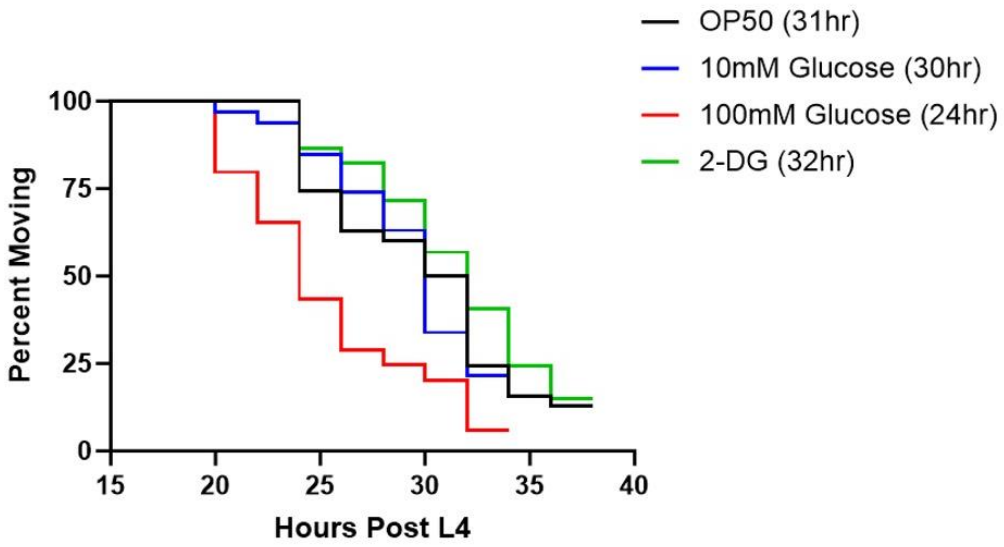

Figure 24: Glucose Must be Metabolized by *C. elegans* to Induce a Shift. Aβ animals grown on NGM agar plates seeded with OP50 *E. coli* were directly grown with nutrient supplementation before seeding. Under these conditions, only 100 mM glucose supplementation, but not 10 mM glucose or 2-DG, which can't be metabolized, decreases the time to Aβ-induced paralysis.

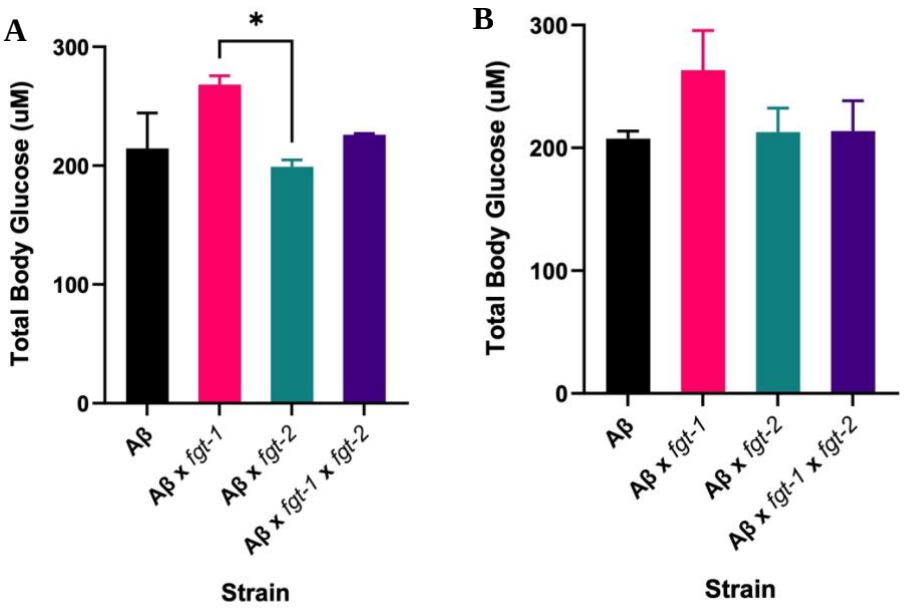

Figure 25: Glucose Supplementation had No Impact on Total Body Glucose. (A) Total body glucose in animals grown on plates seeded with OP50 bacterial culture. *fgt-1* mutants exhibit significantly higher levels of glucose compared to *fgt-2* (*p<0.05). n=2. **(B)** Total body glucose in animals grown on plates seeded with OP50 + 100mM glucose bacterial culture. n=2; total glucose between all strains was not significant when plates were supplemented with glucose.

Chapter 4 DISCUSSION

Impaired glucose metabolism has been implicated as a major symptom and potentiator of Alzheimer's Disease. Because sugar has become increasingly prevalent in the human diet, it is important to study the impact of glucose toxicity on diseases presenting with an inability to correctly process excessive quantities. Considering the links found between type 2 diabetes patients and Alzheimer's, diet is one factor that can influence this disease. Previous work in the lab showcased this ideology as different strains of *E. coli* influenced various AD-like pathogenic features seen in our AD model, such as ATP levels, ROS accumulation, and Aβ-induced paralysis. Taking a closer look into the effect dietary factors can have on disease pathology/symptoms can help us to better understand what makes certain multifactorial conditions tick.

The purpose of my project was to further investigate results we had previously acquired regarding glucose supplementation. We found that the *E. coli* strain HB101 had a protective effect on our Aβ animals versus the standard OP50 *E. coli.* Dr. Andy Lam observed a delayed time-to-paralysis, decreased levels of hydrogen peroxide and superoxide, and increased amounts of available ATP in animals fed HB101 (Lam et al., 2021). These differences displayed between the two diets begged the question regarding what one strain offered that the other did not. Investigation into the macronutrient profiles of OP50 and HB101 led to performing paralysis assays using supplementation with each of the three major nutrients: proteins, lipids, and carbohydrates.

Of the three, the only macronutrient that created a differential effect was glucose, which accelerated the time-to-paralysis significantly. This was then abrogated when animas were fed HB101 + glucose. Although further analysis proved the micronutrient vitamin B_{12} to be a major protective factor, we still wanted to explore the detrimental impact of sugar and HB101's negation.

Originally, we hypothesized that vitamin B_{12} was also the protective factor in HB101 that delayed paralysis in animals fed a high glucose diet. Performing paralysis and ROS assays with OP50 on agar plates supplemented with either 10mM glucose, 148 nM vitamin B_{12}, or 10mM glucose + 148 nM vitamin B_{12} gave interesting results. I was surprised to see that while the addition of B_{12} was slightly beneficial on median paralysis for animals grown with 10mM glucose, it was nowhere near the amount of protection HB101 was able to provide. This mild delay in time-to-paralysis may be explainable when factoring in the hydrogen peroxide results as vitamin B_{12} was able to bring glucose-induced oxidative stress back to control levels. As shown previously, oxidative stress is just one of several factors implicated in the progression and presentation of Alzheimer's Disease; the ability of this micronutrient to combat rising levels of reactive oxygen species is one plausible explanation. However, when throwing glucose into the mix, we must consider that alternative pathways may be triggered.

We know that dietary regulation can impact gene expression depending on the nutrients consumed, such as that of carbohydrates upregulating transcription factors responsible for lipogenesis (Lee et al., 2008), and therefore must consider changes that occur on a genetic level. A previous graduate student in the lab, Kirsten Kervin, performed RNA sequencing on Aβ animals fed OP50 and HB101 fed animals. These

RNASeq data revealed various differentially regulated genes involved in lipid synthesis, stress response, and other integral metabolic processes like glycolysis. HB101 fed animals saw downregulation of *fgt-2*, a glucose transporter, which directly led to my thesis project. Knockdown of *fgt-2* provided staggering results – protection in time-to-paralysis like that of HB101 regardless of the *E. coli* strain animals were fed. When considering the role *fgt-2* plays as an ortholog of the human GLUT1 transporter, we can hypothesize why loss of function may be beneficial. In humans, GLUT1 is responsible for basal glucose uptake and is ubiquitous in expression throughout all cell types (Mueckler et al., 1985). In times of high dietary glucose, this transporter works in overdrive to aid in glucose delivery, storage, and catabolism to return blood sugar to normal – however, it doesn't have nearly as high an affinity to glucose as the GLUT3 transporter. Despite possessing identical substrate binding pockets, GLUT3 is nearly six-times more likely to have glucose binding than GLUT1 (Custódio et al., 2021). GLUT1 cell expression is highest in the neurons and high-energy demand cell types or tissues, which leads me to believe that loss of function in GLUT3 may put more emphasis on this transporter to perform.

It may be possible that in *C. elegans* the loss of *fgt-2* provides cells protection against excessive basal glucose uptake while allowing other sugar transporters to function at a higher capacity than normal, specifically high-energy demand cell types that require more glucose to synthesize fuel. This pathway can be better visualized using a real-life compensation model. Similar to what is seen after closing a major highway, an increase in traffic towards other "neighborhoods" with better, more efficient roads slows the influx to a manageable level. This model could potentially explain why loss of *fgt-2* increased ATP levels. Looking into the expression pattern of

fgt-2 could also explain this protective impact, as it was seen within the body wall muscles where the toxic amyloid-beta peptide is expressed. It is plausible to insinuate that loss of *fgt-2* in this cell-type prevents the negative impact glucose toxicity causes. Further experimentation is needed to observe whether cell-specific rescue will restore the phenotype typically seen in Aβ animals.

My theory is further strengthened when considering the work completed using *fgt-1*, the primary glucose transporter for *C. elegans* and the human GLUT3 homolog. Knockdown of *fgt-1* induced a shift left in time-to-paralysis, the acceleration performing like control animals fed 10mM glucose. As with *fgt-2* mutants, the addition of glucose with OP50 fed animals did not create a significant change in median paralysis, indicating that loss of this gene is involved in modulating glucose metabolism. It is important to note that loss of *fgt-1* is detrimental to Aβ-induced paralysis in animals fed both OP50 and HB101, however addition of 10mM glucose delayed paralysis in the *fgt-1*; Aβ animals grown on HB101 *E. coli.* This restoration contradicts the idea that *fgt-1* is necessary for protection via over stimulus when *fgt-2* is downregulated. However, this doesn't necessarily mean that the model is completely incorrect. Glucose restoring protection suggests that *fgt-1* isn't infallible or as essential as previously imagined and that there may be a compensatory mechanism that can be glucose triggered.

The solute-carrying transport family is one of the largest transmembrane transporters characterized, where *fgt-1* and *fgt-2* are just a two of several identified homologs involved in sugar uptake, suggesting that other solute-carriers may be at play. Another theory is that it may be an impact glucose has on other cellular functions such as plasma membrane (PM) permeability and rigidity response, based off our

knowledge of glucose's downstream effects. It is important to note that not all sugars are the same – they come in different forms such as sucrose, fructose, dextrose, etc. and not all transporters allow each of these solutes to pass. Brooks *et. al* showed that OP50 and HB101 varied in their macronutrient profiles significantly, as OP50 has higher levels of fatty acids but lower carbohydrates versus HB101 (Brooks et al., 2009). Specific characterization of the carbohydrates within HB101 has not been done, but would provide a wealth of information regarding types of sugars in these *E. coli* strains. Although this strain has a lower fatty acid profile, lipid metabolism genes were upregulated in animals grown on this high-sugar culture. This leads me to believe that fatty acid metabolism may be more involved with glucose than previously imagined.

This would be the most plausible, considering the role glucose plays in PM composition through PAQR-2 and IGLR-2 fluidity sensors (Svensk et al., 2016). Svensk *et al.* showed in 2016 that mutant strains for these two sensors are glucose sensitive and significantly decrease membrane fluidity in the molecule's presence. Theoretically, loss of *fgt-1* would cause an imbalance in the sugar concentration gradient (as seen in Figure 25a) and decrease membrane fluidity through these sensors – therefore decreasing overall stress response. If the other sugar transporters are like what we typically see in ion-gated transport where a certain threshold must be met before activation (Gunter & Pfeiffer, 1990), then a hypothesis can be made that the addition of glucose to the high-carbohydrate HB101 restores import/export through recruitment of other transporters.

My preliminary glucose uptake assay results give some insightful results as of now. Interestingly, there was no significant change between my OP50 plates and 100mM glucose plates for all strains, but there was a significant difference (*$p<0.05$)

between my *fgt-1* and *fgt-2* mutants. I will need to conduct the glucose uptake experiment in order to determine whether uptake is changing with supplementation.

The double mutant provides some context regarding what may potentially be occurring. The loss of both *fgt-1* and *fgt-2* causes animals to present with the *fgt-1* phenotype of accelerated time-to-paralysis when fed OP50 and OP50 + glucose. Whether or not loss of *fgt-2* requires *fgt-1* for protection or if loss of *fgt-1* is too great to overcome is unclear; however, considering the previous results showing the acceleration in time-to-paralysis in *fgt-1* animals fed HB101, we can hypothesize that knockdown may hinder loss of *fgt-2*'s positive response to another element within that strain, as HB101 causes downregulation of *fgt-2* on its own. Experimentation with my double mutant on HB101 has not been performed, though, and will be necessary to confirm this suspicion. However, in leu of the RNA sequencing results indicating HB101's impact on *fgt-2* expression, it is a good baseline to consider. All the above these results leave several directions for future experimentation that may shine a light on the interplay between dietary interactions, nutrient metabolism, and AD pathology.

REFERENCES

Anantharaman, M., Tangpong, J., Keller, J. N., Murphy, M. P., Markesbery, W. R., Kiningham, K. K., & St. Clair, D. K. (2006). β-amyloid mediated nitration of manganese superoxide dismutase: Implication for oxidative stress in a APPNLh/NLh X PS-1 P264L/P264L double knock-in mouse model of Alzheimer's disease. *American Journal of Pathology*, *168*(5). https://doi.org/10.2353/ajpath.2006.051223

Ballarini, T., van Lent, D. M., Brunner, J., Schröder, A., Wolfsgruber, S., Altenstein, S., Brosseron, F., Buerger, K., Dechent, P., Dobisch, L., Düzel, E., Ertl-Wagner, B., Fliessbach, K., Freiesleben, S. D., Frommann, I., Glanz, W., Hauser, D., Haynes, J. D., Heneka, M. T., … Wagner, M. (2021). Mediterranean Diet, Alzheimer Disease Biomarkers, and Brain Atrophy in Old Age. *Neurology*, *96*(24). https://doi.org/10.1212/WNL.0000000000012067

Barstead, R., Moulder, G., Cobb, B., Frazee, S., Henthorn, D., Holmes, J., Jerebie, D., Landsdale, M., Osborn, J., Pritchett, C., Robertson, J., Rummage, J., Stokes, E., Vishwanathan, M., Mitani, S., Gengyo-Ando, K., Funatsu, O., Hori, S., Imae, R., … Zapf, R. (2012). Large-scale screening for targeted knockouts in the caenorhabditis elegans genome. *G3: Genes, Genomes, Genetics*, *2*(11). https://doi.org/10.1534/g3.112.003830

Brenner, S. (1974). The genetics of Caenorhabditis elegans. *Genetics*, *77*(1). https://doi.org/10.1093/genetics/77.1.71

Brooks, K. K., Liang, B., & Watts, J. L. (2009). The influence of bacterial diet on fat storage in C. elegans. *PLoS ONE*, *4*(10). https://doi.org/10.1371/journal.pone.0007545

Budson, A. E., & Solomon, P. R. (2012). New criteria for Alzheimer disease and mild cognitive impairment: Implications for the practicing clinician. In *Neurologist* (Vol. 18, Issue 6). https://doi.org/10.1097/NRL.0b013e31826a998d

Butterfield, D. A., & Halliwell, B. (2019). Oxidative stress, dysfunctional glucose metabolism and Alzheimer disease. In *Nature Reviews Neuroscience* (Vol. 20, Issue 3). https://doi.org/10.1038/s41583-019-0132-6

Carter, J., & Lippa, C. (2005). ß-Amyloid, Neuronal Death and Alzheimers Disease. *Current Molecular Medicine*, *1*(6). https://doi.org/10.2174/1566524013363177

Chen, Z., & Zhong, C. (2014). Oxidative stress in Alzheimer's disease. In *Neuroscience Bulletin* (Vol. 30, Issue 2). https://doi.org/10.1007/s12264-013-1423-y

Cioffi, F., Adam, R. H. I., & Broersen, K. (2019). Molecular Mechanisms and Genetics of Oxidative Stress in Alzheimer's Disease. In *Journal of Alzheimer's Disease* (Vol. 72, Issue 4). https://doi.org/10.3233/JAD-190863

Custódio, T. F., Paulsen, P. A., Frain, K. M., & Pedersen, B. P. (2021). Structural comparison of GLUT1 to GLUT3 reveal transport regulation mechanism in sugar porter family. *Life Science Alliance*, *4*(4). https://doi.org/10.26508/LSA.202000858

D'Andrea Meira, I., Romão, T. T., Do Prado, H. J. P., Krüger, L. T., Pires, M. E. P., & Da Conceição, P. O. (2019). Ketogenic diet and epilepsy: What we know so far. *Frontiers in Neuroscience*, *13*(JAN). https://doi.org/10.3389/fnins.2019.00005

Deshpande, A., Mina, E., Glabe, C., & Busciglio, J. (2006). Different conformations of amyloid β induce neurotoxicity by distinct mechanisms in human cortical neurons. *Journal of Neuroscience*, *26*(22). https://doi.org/10.1523/JNEUROSCI.1189-06.2006

Deture, M. A., & Dickson, D. W. (2019). The neuropathological diagnosis of Alzheimer's disease. In *Molecular Neurodegeneration* (Vol. 14, Issue 1). https://doi.org/10.1186/s13024-019-0333-5

Garde, A., Kenny, I. W., Kelley, L. C., Chi, Q., Mutlu, A. S., Wang, M. C., & Sherwood, D. R. (2022). Localized glucose import, glycolytic processing, and mitochondria generate a focused ATP burst to power basement-membrane invasion. *Developmental Cell*, *57*(6). https://doi.org/10.1016/j.devcel.2022.02.019

Giraldo, E., Lloret, A., Fuchsberger, T., & Viña, J. (2014). Aβ and tau toxicities in Alzheimer's are linked via oxidative stress-induced p38 activation: Protective role of vitamin E. *Redox Biology*, *2*(1). https://doi.org/10.1016/j.redox.2014.03.002

Grammatikopoulou, M. G., Goulis, D. G., Gkiouras, K., Theodoridis, X., Gkouskou, K. K., Evangeliou, A., Dardiotis, E., & Bogdanos, D. P. (2020). To Keto or Not to Keto? A Systematic Review of Randomized Controlled Trials Assessing the Effects of Ketogenic Therapy on Alzheimer Disease. In *Advances in Nutrition* (Vol. 11, Issue 6). https://doi.org/10.1093/advances/nmaa073

Gunter, T. E., & Pfeiffer, D. R. (1990). Mechanisms by which mitochondria transport calcium. In *American Journal of Physiology - Cell Physiology* (Vol. 258, Issues 5 27-5). https://doi.org/10.1152/ajpcell.1990.258.5.c755

Hampel, H., Mesulam, M. M., Cuello, A. C., Farlow, M. R., Giacobini, E., Grossberg, G. T., Khachaturian, A. S., Vergallo, A., Cavedo, E., Snyder, P. J., & Khachaturian, Z. S. (2018). The cholinergic system in the pathophysiology and treatment of Alzheimer's disease. In *Brain* (Vol. 141, Issue 7). https://doi.org/10.1093/brain/awy132

Hardy, J., & Allsop, D. (1991). Amyloid deposition as the central event in the aetiology of Alzheimer's disease. In *Trends in Pharmacological Sciences* (Vol. 12, Issue C). https://doi.org/10.1016/0165-6147(91)90609-V

Hardy, J., & Selkoe, D. J. (2002). The amyloid hypothesis of Alzheimer's disease: Progress and problems on the road to therapeutics. In *Science* (Vol. 297, Issue 5580). https://doi.org/10.1126/science.1072994

Houstis, N., Rosen, E. D., & Lander, E. S. (2006). Reactive oxygen species have a causal role in multiple forms of insulin resistance. *Nature*, *440*(7086). https://doi.org/10.1038/nature04634

Institute of Medicine. (2005). Dietary Reference Intakes for Energy, Carbohydrate, Fiber, Fat, Fatty Acids, Cholesterol, Protein, and Amino Acids (Macronutrients) Washington, DC: The National Academies Press. https://doi.org/10.17226/10490. Visit. In *Dietary Reference Intakes for Energy, Carbohydrate, Fiber, Fat, Fatty Acids, Cholesterol, Protein, and Amino Acids (Macronutrients)*.

Jansen, I. E., Savage, J. E., Watanabe, K., Bryois, J., Williams, D. M., Steinberg, S., Sealock, J., Karlsson, I. K., Hägg, S., Athanasiu, L., Voyle, N., Proitsi, P., Witoelar, A., Stringer, S., Aarsland, D., Almdahl, I. S., Andersen, F., Bergh, S., Bettella, F., … Posthuma, D. (2019). Genome-wide meta-analysis identifies new loci and functional pathways influencing Alzheimer's disease risk. *Nature Genetics*, *51*(3). https://doi.org/10.1038/s41588-018-0311-9

Karch, C. M., & Goate, A. M. (2015). Alzheimer's disease risk genes and mechanisms of disease pathogenesis. In *Biological Psychiatry* (Vol. 77, Issue 1). https://doi.org/10.1016/j.biopsych.2014.05.006

Kehm, R., Baldensperger, T., Raupbach, J., & Höhn, A. (2021). Protein oxidation - Formation mechanisms, detection and relevance as biomarkers in human diseases. In *Redox Biology* (Vol. 42). https://doi.org/10.1016/j.redox.2021.101901

Keller, J. N., Schmitt, F. A., Scheff, S. W., Ding, Q., Chen, Q., Butterfield, D. A., & Markesbery, W. R. (2005). Evidence of increased oxidative damage in subjects with mild cognitive impairment. *Neurology*, *64*(7). https://doi.org/10.1212/01.WNL.0000156156.13641.BA

Kenyon, C., Chang, J., Gensch, E., Rudner, A., & Tabtiang, R. (1993). A C. elegans mutant that lives twice as long as wild type. *Nature*, *366*(6454). https://doi.org/10.1038/366461a0

King, E. A., Wade Davis, J., & Degner, J. F. (2019). Are drug targets with genetic support twice as likely to be approved? Revised estimates of the impact of genetic support for drug mechanisms on the probability of drug approval. *PLoS Genetics*, *15*(12). https://doi.org/10.1371/journal.pgen.1008489

Koepsell, H. (2020). Glucose transporters in brain in health and disease. In *Pflugers Archiv European Journal of Physiology* (Vol. 472, Issue 9). https://doi.org/10.1007/s00424-020-02441-x

Lai, C. H., Chou, C. Y., Ch'ang, L. Y., Liu, C. S., & Lin, W. C. (2000). Identification of novel human genes evolutionarily conserved in Caenorhabditis elegans by comparative proteomics. *Genome Research*, *10*(5). https://doi.org/10.1101/gr.10.5.703

Lam, A. B., Kervin, K., & Tanis, J. E. (2021). Vitamin B12 impacts amyloid beta-induced proteotoxicity by regulating the methionine/S-adenosylmethionine cycle. *Cell Reports*, *36*(13). https://doi.org/10.1016/j.celrep.2021.109753

Lane, C. A., Hardy, J., & Schott, J. M. (2018). Alzheimer's disease. In *European Journal of Neurology* (Vol. 25, Issue 1). https://doi.org/10.1111/ene.13439

Lee, A. H., Scapa, E. F., Cohen, D. E., & Glimcher, L. H. (2008). Regulation of hepatic lipogenesis by the transcription factor XBP1. *Science*, *320*(5882). https://doi.org/10.1126/science.1158042

Litke, R., Garcharna, L. C., Jiwani, S., & Neugroschl, J. (2021). Modifiable Risk Factors in Alzheimer Disease and Related Dementias: A Review. In *Clinical Therapeutics* (Vol. 43, Issue 6). https://doi.org/10.1016/j.clinthera.2021.05.006

Maillot, M., Vieux, F., Amiot, M. J., & Darmon, N. (2010). Individual diet modeling translates nutrient recommendations into realistic and individual-specific food choices. *American Journal of Clinical Nutrition*, *91*(2). https://doi.org/10.3945/ajcn.2009.28426

Malone, J. I., & Hansen, B. C. (2019). Does obesity cause type 2 diabetes mellitus (T2DM)? Or is it the opposite? In *Pediatric Diabetes* (Vol. 20, Issue 1). https://doi.org/10.1111/pedi.12787

Manczak, M., Anekonda, T. S., Henson, E., Park, B. S., Quinn, J., & Reddy, P. H. (2006). Mitochondria are a direct site of Aβ accumulation in Alzheimer's disease neurons: Implications for free radical generation and oxidative damage in disease progression. *Human Molecular Genetics*, *15*(9). https://doi.org/10.1093/hmg/ddl066

Mueckler, M., Caruso, C., Baldwin, S. A., Panico, M., Blench, I., Morris, H. R., Allard, W. J., Lienhard, G. E., & Lodish, H. F. (1985). Sequence and structure of a human glucose transporter. *Science*, *229*(4717). https://doi.org/10.1126/science.3839598

Muschiol, D., Schroeder, F., & Traunspurger, W. (2009). Life cycle and population growth rate of Caenorhabditis elegans studied by a new method. *BMC Ecology*, *9*. https://doi.org/10.1186/1472-6785-9-14

Navale, A. M., & Paranjape, A. N. (2016). Glucose transporters: physiological and pathological roles. In *Biophysical Reviews* (Vol. 8, Issue 1). https://doi.org/10.1007/s12551-015-0186-2

O'Brien, R. J., & Wong, P. C. (2011). Amyloid precursor protein processing and alzheimer's disease. *Annual Review of Neuroscience*, *34*. https://doi.org/10.1146/annurev-neuro-061010-113613

Oda, T., Wals, P., Osterburg, H. H., Johnson, S. A., Pasinetti, G. M., Morgan, T. E., Rozovsky, I., Stine, W. B., Snyder, S. W., Holzman, T. F., Krafft, G. A., & Finch, C. E. (1995). Clusterin (apoJ) alters the aggregation of amyloid β-peptide (Aβ1-42) and forms slowly sedimenting aβ complexes that cause oxidative stress. *Experimental Neurology*, *136*(1). https://doi.org/10.1006/exnr.1995.1080

O'Neill, B., & Raggi, P. (2020). The ketogenic diet: Pros and cons. In *Atherosclerosis* (Vol. 292). https://doi.org/10.1016/j.atherosclerosis.2019.11.021

Reitz, C., Rogaeva, E., & Beecham, G. W. (2020). Late-onset vs nonmendelian early-onset Alzheimer disease. *Neurology Genetics*, *6*(5). https://doi.org/10.1212/nxg.0000000000000512

Rosa, R. De, Spinozzi, F., & Itri, R. (2018). Hydroperoxide and carboxyl groups preferential location in oxidized biomembranes experimentally determined by small angle X-ray scattering: Implications in membrane structure. *Biochimica et Biophysica Acta - Biomembranes*, *1860*(11). https://doi.org/10.1016/j.bbamem.2018.05.011

Saltiel, A. R., & Kahn, C. R. (2001). Insulin signalling and the regulation of glucose and lipid metabolism. In *Nature* (Vol. 414, Issue 6865). https://doi.org/10.1038/414799a

Scarmeas, N., Luchsinger, J. A., Schupf, N., Brickman, A. M., Cosentino, S., Tang, M. X., & Stern, Y. (2009). Physical activity, diet, and risk of Alzheimer disease. *JAMA*, *302*(6). https://doi.org/10.1001/jama.2009.1144

Scheuner, D., Eckman, C., Jensen, M., Song, X., Citron, M., Suzuki, N., Bird, T. D., Hardy, J., Hutton, M., Kukull, W., Larson, E., Levy-Lahad, E., Viitanen, M., Peskind, E., Poorkaj, P., Schellenberg, G., Tanzi, R., Wasco, W., Lannfelt, L., … Younkin, S. (1996). Secreted amyloid β-protein similar to that in the senile plaques of Alzheimer's disease is increased in vivo by the presenilin 1 and 2 and APP mutations linked to familial Alzheimer's disease. *Nature Medicine*, *2*(8). https://doi.org/10.1038/nm0896-864

Schmechel, D. E., Saunders, A. M., Strittmatter, W. J., Crain, B. J., Hulette, C. M., Joo, S. H., Pericak-Vance, M. A., Goldgaber, D., & Roses, A. D. (1993). Increased amyloid β-peptide deposition in cerebral cortex as a consequence of apolipoprotein E genotype in late-onset Alzheimer disease. *Proceedings of the National Academy of Sciences of the United States of America*, *90*(20). https://doi.org/10.1073/pnas.90.20.9649

Selkoe, D. J. (1994). Cell biology of the amyloid β-protein precursor and the mechanism of Alzheimer's disease. In *Annual Review of Cell Biology* (Vol. 10). https://doi.org/10.1146/annurev.cb.10.110194.002105

Shaye, D. D., & Greenwald, I. (2011). Ortholist: A compendium of C. elegans genes with human orthologs. *PLoS ONE*, *6*(5). https://doi.org/10.1371/journal.pone.0020085

Snyder, S. W., Ladror, U. S., Wade, W. S., Wang, G. T., Barrett, L. W., Matayoshi, E. D., Huffaker, H. J., Krafft, G. A., & Holzman, T. F. (1994). Amyloid-beta aggregation: selective inhibition of aggregation in mixtures of amyloid with different chain lengths. *Biophysical Journal*, *67*(3). https://doi.org/10.1016/S0006-3495(94)80591-0

Svensk, E., Devkota, R., Ståhlman, M., Ranji, P., Rauthan, M., Magnusson, F., Hammarsten, S., Johansson, M., Borén, J., & Pilon, M. (2016). Caenorhabditis elegans PAQR-2 and IGLR-2 Protect against Glucose Toxicity by Modulating Membrane Lipid Composition. *PLoS Genetics*, *12*(4). https://doi.org/10.1371/journal.pgen.1005982

Weller, J., & Budson, A. (2018). Current understanding of Alzheimer's disease diagnosis and treatment. In *F1000Research* (Vol. 7). https://doi.org/10.12688/f1000research.14506.1

Wong-Ekkabut, J., Xu, Z., Triampo, W., Tang, I. M., Tieleman, D. P., & Monticelli, L. (2007). Effect of lipid peroxidation on the properties of lipid bilayers: A molecular dynamics study. *Biophysical Journal*, *93*(12). https://doi.org/10.1529/biophysj.107.112565

Yilmaz, L. S., & Walhout, A. J. M. (2014). Worms, bacteria, and micronutrients: An elegant model of our diet. In *Trends in Genetics* (Vol. 30, Issue 11). https://doi.org/10.1016/j.tig.2014.07.010

Zhang, X. X., Tian, Y., Wang, Z. T., Ma, Y. H., Tan, L., & Yu, J. T. (2021). The Epidemiology of Alzheimer's Disease Modifiable Risk Factors and Prevention. In *Journal of Prevention of Alzheimer's Disease* (Vol. 8, Issue 3). https://doi.org/10.14283/jpad.2021.15